AFRL-OSR-VA-TR-2014-0347

Creation of an Aeronautical Capstone

Anthony Luscher
OHIO STATE UNIVERSITY THE

12/08/2014
Final Report

Air Force Research Laboratory
AF Office Of Scientific Research (AFOSR)/ RTB
Arlington, Virginia 22203
Air Force Materiel Command

REPORT DOCUMENTATION PAGE

Form Approved
OMB No. 0704-0188

1. REPORT DATE *(DD-MM-YYYY)*
12-11-2014

2. REPORT TYPE
FINAL PERFORMANCE REPORT

3. DATES COVERED *(From - To)*
1 AUGUST 2011 - 31 JULY 2014

4. TITLE AND SUBTITLE
CREATION OF AN AERONAUTICAL CAPSTONE DESIGN PROJECT PROGRAM AT OHIO STATE UNIVERSITY
FINAL PERFORMANCE REPORT

5a. CONTRACT NUMBER

5b. GRANT NUMBER
FA9550-11-1-0214

5c. PROGRAM ELEMENT NUMBER

6. AUTHOR(S)
LUSCHER, ANTHONY, F

5d. PROJECT NUMBER

5e. TASK NUMBER

5f. WORK UNIT NUMBER

7. PERFORMING ORGANIZATION NAME(S) AND ADDRESS(ES)
OHIO STATE UNIVERSITY, THE
DEPARTMENT OF MECHANICAL AND AEROSPACE ENGINEERING
201 W. 19TH AVE
COLUMBUS, OH 43210

8. PERFORMING ORGANIZATION REPORT NUMBER

9. SPONSORING / MONITORING AGENCY NAME(S) AND ADDRESS(ES)
USAF, AFRL DUNS 143574726
AF OFFICE OF SCIENTIFIC RESEARCH
875 N. RANDOLPH ST. ROOM 3112
ARLINGTON, VA 22203

10. SPONSOR/MONITOR'S ACRONYM(S)
USAF AFRL

11. SPONSOR/MONITOR'S REPORT NUMBER(S)

12. DISTRIBUTION / AVAILABILITY STATEMENT
DISTRIBUTION A

13. SUPPLEMENTARY NOTES

14. ABSTRACT
THIS PROJECT ALLOWED STUDENS FROM THE DEPARTMENT OF MECHANICAL ENGINEERING AT THE OHIO STATE UNIVERSITY TO COMPETE IN THE AFRL UNIVERSITY CHALLENGE PROJECT. THESE YEARLY PROJECTS PROVIDED AN
INVALUABLE EXPERIENCE FOR OUR CAPSTONE STUDENTS. APPROXIMATELY 90 DESIGN STUDENTS CONTRIBUTED TO THE
CONCEPTUAL DESIGN OF THE PROJECTS FOR THE FIRST 2 YEARS. STUDENTS BENEFITED FROM UNDERSTANDING THE
PROBLEM, DEVELOPING INNOVATIVE CONCEPTS AND PROPOSING DETAILED SOLUTIONS. SMALLER TEAMS OF STUDENTS
COMPLETED THE FINAL PROJECTS FOR THESE FIRST 2 YEARS. FOR THE 3RD YEAR A 7-STUDENT TEAM WORKED 6.5 MONTHS
ON CREATING A SOLUTION. STUDENTS BENEFITED GREATLY FROM TRAVELING TO THE EVENT AND

15. SUBJECT TERMS

16. SECURITY CLASSIFICATION OF:			17. LIMITATION OF ABSTRACT	18. NUMBER OF PAGES	19a. NAME OF RESPONSIBLE PERSON
a. REPORT	**b. ABSTRACT**	**c. THIS PAGE**	SAR	122	LUSCHER, ANTHONY, F
					19b. TELEPHONE NUMBER *(include area code)* (614) 292-4474

Creation of an Aeronautical Capstone Design Project Program at Ohio State University

Final Performance Report

Anthony F. Luscher

12 November, 2014

Grant Number: FA9550-11-1-0214

THE OHIO STATE UNIVERSITY
DEPARTMENT OF MECHANICAL AND AEROSPACE ENGINEERING
201 W. 19TH AVE
COLUMBUS, OH 43210

Abstract

This project allowed students from the Department of Mechanical Engineering at The Ohio State University to compete in the AFRL University Challenge Project. These yearly projects provided an invaluable experience for our capstone students. Approximately 90 design students contributed to the conceptual design of the projects for the first 2 years. Students benefited from understanding the problem, developing innovative concepts and proposing detailed solutions. Smaller teams of students completed the final projects for these first two years. For the 3rd year a 7 student team worked 6.5 months on creating a solution. Students benefited greatly from traveling to the event and participating in the competition. The project benefited the teaching of design in our capstone design program.

This report summarizes 3 projects that were completed by the capstone design teams at Ohio State in the Department of Mechanical and Aerospace Engineering.

2013-2014 AFRL University Design Project: Heavy Lift

The project was to create a heavy lift kit for use by members of the USAF Special Tactics "Pararescue" (PJ) community. The objective was to develop a system that was man-portable (lightweight and packable) and easily set up/used by a single operator. The goal was to lift 45K lbs. at least 18 inches. The student team created a portable air bag system that worked very well. Below is a picture of the Ohio State student team's entry lifting a Caterpillar D6 bulldozer. The OSU team did very well and was able to lift the tractor over 26 inches. The students contributed to the AFRL's understanding of the problem.

Ohio State University Student Team's Heavy Lift Airbag Under Testing

2012-2013 AFRL University Design Project: Portable Bridging System

The project was to create a portable bridging system for use by members of the USAF Special Tactics "Pararescue" (PJ) community. These airmen need a more reliable way to cross canals, get from roof top to roof top and cross any aforementioned gap encountered on a mission. Solutions were requested to be lightweight, have a multipurpose role, be easy to deploy, reusable, and easy to maintain. The OSU team created a structure that could be stick built from a single carbon fiber and aluminum attachment structure. The attachment system was novel and provided strength as well as quick assembly. The design was extremely portable and was successful with the OSU teaming coming in second place at the competition.

Ohio State University Student Team's Portable Bridging Design Under Testing

2011-2012 AFRL University Design Project: Assault Climbing Device

The project was to create a method of having a lead person rapidly climb a vertical structure and lay ropes for follow-on climbers. The attachment points for the structure needed to be fired from 90 feet away from the structure. The OSU team created a variety of solutions for attaching ropes to the vertical concrete structure. None of these were able to be deployed and the OSU team was not able to compete.

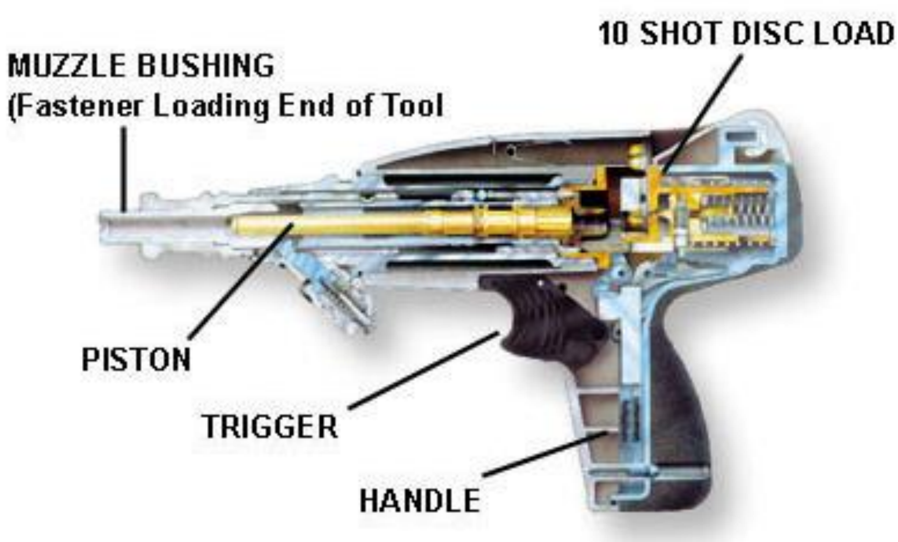

2014 Ohio State University AFRL Design Challenge

Presented on 4/15 /14 at Arnold Air Force Base in Manchester, TN

Students:

Nick Ernst
Trevin Fondriest
Alex Hart
Daniel Hunker
Greg Ward

GTAs:

Ilia Gotlib
Tim Seitz

Advisor:

Dr. Anthony Luscher

Table of Contents

Executive Summary

Battlefield Airmen depend on their equipment for their safety and the success of their missions. During rescue operations, airmen have experienced difficulty lifting downed vehicles in order to retrieve personnel and equipment. To face this obstacle, ground forces need a lightweight portable device capable of lifting large weights. During the design process, Major Joseph Barnard and Chief Master Sergeant Ryan Schultz provided insight on the needs of para-jumping airmen.

This report examines every detail of the design and analysis of the lift solution submitted by The Ohio State University. In order to lift a 55,000 pound vehicle, the team investigated many conceptual designs and suggests using an air bag pressurized according to the area of lift. Important constraints such as weight, volume, and lift capacity are explored. Common modes of failure are analyzed, while solutions and precautions are explained. For any design to be successful, extensive testing is necessary. Thorough description of all tests is provided, proving the validity of the design concept.

The contents of the Heavy REDs extraction pack include air bags and compressed air tanks. The Ohio State University's solution includes a single air bag and air tank. Not only is the number of components slimmed down, the team added a top plate that better distributes the load. The weight and packed volume of the design goals is considerably compromised. Efforts were concentrated on lifting the desirable object, rated to 60,000 pounds (assuming only half the vehicle weight needs to be lifted due to the physics of the problem). The weight of the top plate is heavier than expected, leaving opportunity for continuous improvement.

The User: Pararescuemen (PJs)

Pararescuemen, or PJs, are United States Air Force Special Operations Command and Air Combat Command operatives who risk their lives to rescue, recover, and provide medical treatment to personnel in combat and humanitarian settings. They are trained in emergency medical tactics, combat, and survival and have the ability to go anywhere necessary to perform their services [1]. PJs are tasked with navigating unfamiliar environments to rescue personnel in need of assistance. Such situations include, but are not limited to, combat personal stuck under overturned vehicles as well as civilians trapped in debris from fallen buildings in natural disaster environments. To perform these rescues, the current solution uses a series of air bags with lift capacity of 10,000 pounds each inflated by a 4500 psi air tank.


Figure 1: PJs arriving on site for a rescue operation

The User's Needs

The PJs are faced with unpredictable rescue missions that require personnel extraction from extreme environments and stress intensive situations. To be able to conduct a safe and successful rescue mission, the current lift system needs to be revamped in multiple areas. Chief Master Sergeant Ryan Schultz and Major Joseph Barnard provided great insight from a first-hand point of view as to what exactly PJs need for their rescue missions.

One of the greatest concerns expressed by Schultz and Barnard was that the solution must be able to perform in extreme terrains and sloppy conditions. Battlefields are often rocky dirt fields with severe slopes and debris scattered about. When a vehicle overturns and fluids such as oil and diesel start to leak, the situation begins to deteriorate quickly. For a solution to be successful it must be deployable in any environment and be protected against sharp objects, slippery surfaces, and various other adverse conditions. Such conditions are illustrated below in Figure 2.

Figure 2 - MRAP after an IED explosion in rocky environment

Shultz and Barnard also expressed the need for a simple solution that could be operated by personnel with very little training or experience. The solution must be easy to operate by users wearing full combat gear including gloves. An ideal solution would require no tools to assembly and all fittings should be easy to fix by hand. A quick and intuitive set-up and lift operation is desirable along with the ability to easily control the height of the lift.

Further needs of the solution include the competition objective goals. Shultz and Barnard emphasized the need for a man portable solution that can achieve a lift height of 24 inches. The solution should be able to lift a vehicle that weighs 45,000 pounds and should require as few iterations as possible. The current system uses multiple 10,000 lift capacity bags to lift heavier vehicles requiring additional set-up time and adjustments.

The current solution is part of a larger Heavy RED kit that includes other rescue equipment such as a concrete saw, Jaws of Life, and a gas generator.

Goals of the Design

Table 1 - Team goals for the solution requirements

Goal	How the goal drove the design
Lift Height	All conceptual designs were based on being able to lift a vehicle 24 inches on one side
Lift Capacity	All conceptual designs would be able to lift a 55000 pound vehicle by tilting the vehicle on a pivot
Usability in Adverse Conditions	Knowing the conditions will almost always be unpredictable, all conceptual designs were designed to perform in various harsh environments
Simplicity	To provide a quick and successful rescue mission, the solution must be easily assembled, require no tools, and be hand operated while wearing gloves

The Air Bag: Overview

The following section details the different components of the design. Further analysis of why each component was chosen till follow in the Detailed Analysis section.

Pneumatic Air Bag

Petersen Products supplied the ballistic nylon rubber pneumatic air bag (Figure 3). The bag is made of ballistic nylon thread that is weaved together to make a single ply. The plies are then stacked together to create the shell of the bag with a thickness of .2 inches. Using multiple plies allows for more elasticity than a similarly thick solid rubber construction. The plies are then covered with a protective nylon cover for abrasion and puncture protection. The pneumatic air bag is of cylindrical shape with a diameter of 24 inches and a height of 24 inches.

Figure 3 - Pneumatic Air Bag

This was the aspect of design with the largest engineering trade off. The larger the diameter of the bag the greater the stability and lower working pressure, but it also meant that the weight and packing volume would be negatively affected. A comprehensive study was done to determine the advantages and disadvantages of bags with three different diameters looking at the required working pressure, aspect ratio, bag thickness, contact area between the bag and object lifted, surface area of the bag, ideal packed volume, and estimated weight to determine the optimal bag for completing the challenge of lifting the object to the required height while minimizing the packed weight, volume, and working pressure as much as possible. Table 2 shows the comparison of the study. The 24 inch diameter by 24 inch height cylindrical bag was chosen as the most optimal bag to suit the needs of the Air Force.

Table 2 - Trade-Off Table

	20” x 24” bag	24” x 24” bag	30” x 24” bag
Force to Lift (lbs)	30,000	30,000	30,000
Required Pressure (psi)	96	67	43
Aspect Ratio (d/h)	.833	1	1.25
Material Thickness (in)	.25	.2	.15
Contact Area (in^2)	314.2	452.4	706.9
Surface Area (in^2)	2136	2714	3676
Ideal Packed Volume (in^3)	534.1	542.9	551.3
Estimated Weight (lbs)	13	16	20

Custom Top Plate

To ensure the maximum amount of surface area from the bag is in contact with the vehicle and to protect the bag from sharp objects, a carbon fiber plate was created. The plate consisted of 7 carbon fiber tubes, 4 aluminum support brackets and 2 Kevlar reinforcement sheets. The assembly is held together with rivets. The general construction is shown in Figure 4. Additionally, to increase the strength of the carbon fiber tubes, the middle 6 inches of each tube was filled with a small wooden plug and a pourable resin.

Figure 4 - Carbon Fiber Top Plate

After testing the top plate's effectiveness, it was clear that the carbon fiber surface was too smooth, causing the plate to slide off of the bag under heavy load. Thus, the top section of the plate was covered with approximately 3/16" of Rhino Liner, seen in Figure 5 below. The additional coating only added approximately 8 ounces and greatly increased the grip and rigidity of the plate.

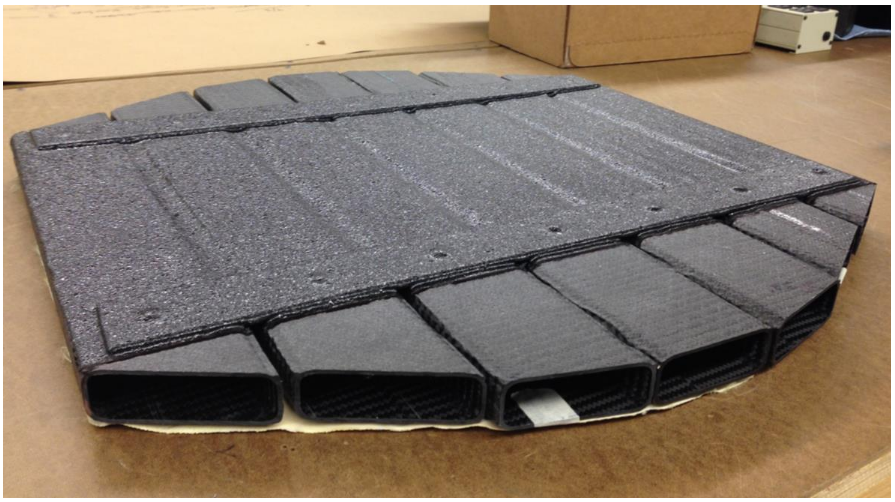

Figure 5 - Completed Top Plate

Bottom Stability & Traction - Stakes

After testing multiple stakes, it was clear that each stake has its own advantages and disadvantages. The standard issue military tent stake performed the best, but required hammering or stomping when inserted into hard grounds. Although this can be done rather easily with a boot or standard issue military shovel, it is impractical in tight conditions. Also, the military tent stakes are easily stacked together, saving on packed volume. The AEA Ground Penetrator was useful in these tight conditions due to the screw shape and T-handle. The ideal packed volume of these stakes is greater than the military tent stake but weighed slightly less. Figure 6 shows both stakes side-by-side.

Figure 6 - Military Tent Stake & Ground Penetrator

A combination of the two stakes will be used with the air bag. Under tight conditions, a maximum of 3 tent stakes will be able to be used. Thus, one military tent stake and two AEA Ground Penetrators are designed to be packed with the bag. Figure 7 shows the stakes and the bag combined.

Figure 7 - Air Bag & Stakes

3/16” thick, black powder-coated steel carabiner connectors hook the military tent stakes to the air bag so they may be pounded into the ground prior to being attached.

Bottom Stability & Traction- Treaded Rubber Mats

Following the meetings with CMSgt Schultz and Maj Barnard, it was brought to the team’s attention that often at crash sites there are tremendous amounts of spilled fuel and oil. As mentioned above, the outer shell of our bag is constructed of multiple plies of a nylon laced fabric. The contact area of the bottom of the bag, in contact with oil, will make the bag want to slip in less than ideal loading conditions. Thus a 1” thick, 24” diameter flexible, grease resistant rubber mat was attached to the bottom of the air bag through the loops. Additionally, the bottom side of the mat has tread that digs into the ground when under heavy loads, improving the air bag’s stability and traction in all terrains. Figure 7, Figure 8, and Figure 9 show the mat attached to the bag, the chosen rubber mat’s tread, and the imprint left into the terrain after lifting a heavy object.

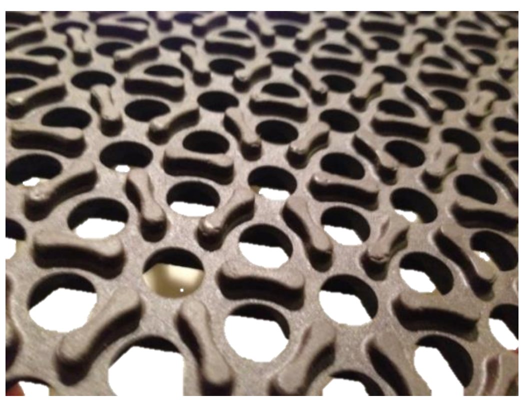

Figure 8 - Tread on Rubber Mat

Figure 9 - Rubber Tread Imprint

Power Supply

To inflate the air bag to the required 66.7 psi a few options were considered for the source of compressed air. The first idea came from the idea of a car air bag. Air bags in cars use a chemical reaction to rapidly generate air to fill the bag and provide a cushion in an impact situation. Significant time was put into researching this topic and in the end it was determined that this method would be very hard to control and would therefore create an unsafe and unstable lifting operation. Along with being unstable, the air bag uses chemicals that can be toxic if not handled properly and could provide a hazard to airmen carrying and using the bag.

The next option that was considered for power supply was a small, handheld, battery-operated air compressor similar to the one shown below in Figure 10. This device is used to inflate car tires in emergency situations. Some models have the capability of reaching 120 psi through a 12V rechargeable battery. This idea seemed fruitful at first however additional research suggested that the batteries would not have a sufficient amount of energy to fully inflate the air bag. With this in mind, it was determined that a much greater amount of energy would be required to lift the bag and thus a compressed air cylinder was selected as the source of power.

Figure 10 - Battery operated air compressor

Compressed air cylinders have the ability to be filled offsite and hold their pressure indefinitely until needed. This is ideal for a rescue operation as you can always have tanks filled and ready to go.

In the search for the right air tank, many bottles were analyzed before settling on a 45-minute SCBA (self-contained breathing apparatus) firefighter bottle. This bottle contains 88 cubic feet of air compressed to 4500 psi in a carbon fiber wrapped aluminum tank. The tank, seen below in Figure 11, includes an easily adjustable regulator and a quick connect valve assembly for easy airline hook-up.

Figure 11 - SCBA 4500 psi air tank

This tank has enough air for 2.75 lifts to allow for multiple lifts on a single deployment. A smaller 30-minute SCBA bottle (45 cubic feet of air at 2216 psi) was used for testing and can be used for 1 lift if desired. The larger bottle was selected for this design to allow for the opportunity to execute multiple lifts on a single deployment and provide a cushion to account for any air lost in set-up or adjustments.

Airline Assembly

To safely fill the bag with the compressed air from the SCBA tank, a series of valves and fitting were attached to the air-line assembly. Starting from the bottle, the first component of the assembly is the easy connect screw. This feature allows the line to be easily connected to the tank without having to turn the entire bottle. It has a large, rough fitting that can easily be turned by hand with or without gloves. This leads into the regulator that allows for the pressure to be reduced to operating pressure (0 - 90 psi). From here the line contains a 100 psi gauge and an adjustable pressure relief valve. These two features allow for the bag pressure to be safely monitored to ensure the bag doesn't overinflate. The adjustable relief valve keeps the system from exceeding 90 psi and can be adjusted all the way down to 0 psi to safely control the lowering stage of the lift operation. Next there is an on/off valve leading to the 12 foot air-line. The on/off valve allows for the bag to remain pressurized without leaking. The 12 feet of line allows for the operator to remain a safe distance away from the air bag/vehicle and is rated to 350 psi to ensure no line rupturing occurs. The line finally connects to the bag via another ½" on/off valve that allows for the bag to remain inflated under the load while the air tank and air-line assembly is disconnected if desired. The final assembly can be seen below in Figure 12.

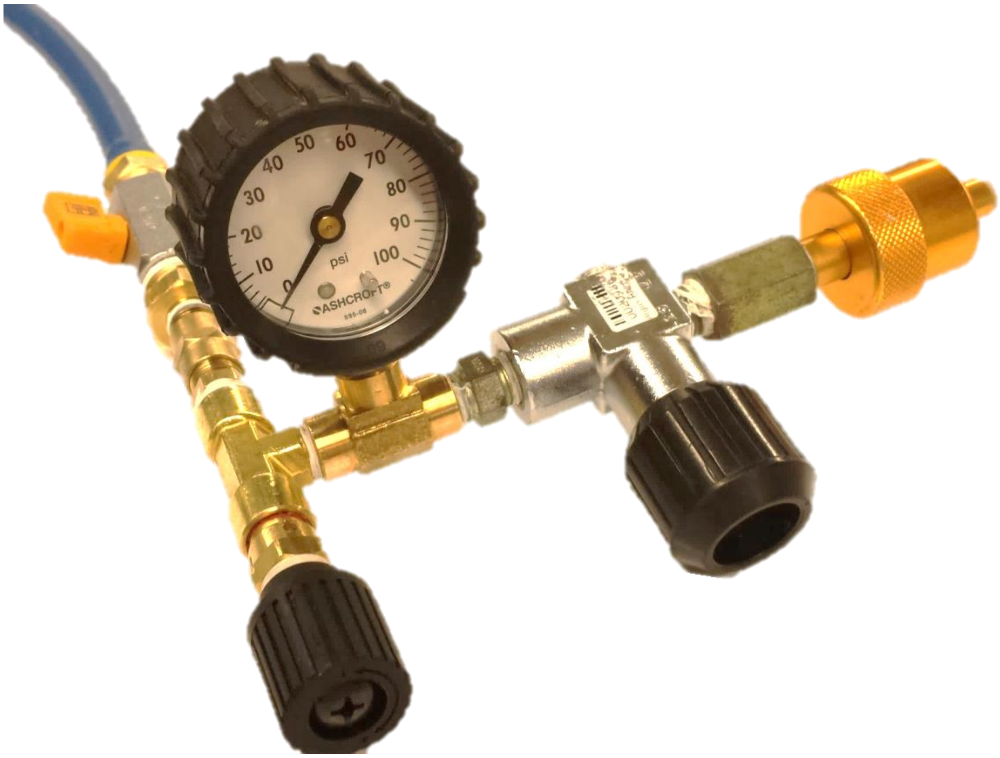

Figure 12 - Airline Assembly

The Air Bag: In Field Use

Upon arrival on site of the rescue operation, the air bag lifting system should be deployed using the steps listed below. These steps can be performed by any crew member and take little to no training other than performing a simple test run to familiarize yourself with the system. The steps are as follows:

1) Have one person begin digging an 8 inch deep hole under the vehicle at the lift point
2) Have the other person unhook the two backpack straps and set the system on the ground
3) Unhook the two opposite side straps to release the air tank and air bag
4) Flatten out airbag and push in the sides
5) Attach top plate to top of airbag by matching up the Velcro
6) Place airbag in approximate location of lift location and take note of stake loops on bottom side
7) Hammer in three stakes and attach to airbag loops using supplied carabiners
8) Attach airline assembly to air tank via the gold hand operated screw valve
9) Ensure regulator on airline assembly is turned all the way clockwise (OFF) and do the same for the adjustable pressure relief valve
10) Make sure both orange ON/OFF valves are parallel with the lines (OPEN)

11) Un screw regulator on tank counter clockwise to allow for pressurization
12) Turn the regulator on the airline assembly counter clockwise to begin filling bag
13) Adjust airline regulator for desired inflation rate and monitor bag pressure using the gauge
14) When full lift height is achieved close regulator valve and turn ON/OFF valve 90 degrees

With the lifting operation now complete, the bag can be kept in place indefinitely by leaving the ON/OFF valves closed. When it comes time to deflate the bag and lower the vehicle, the following steps should be followed:

1) Turn off valve on air tank
2) Open ON/OFF valve
3) Unscrew pressure relief valve to allow for air to escape at an adjustable rate
4) Continue until full deflation and fully open line regulator to bleed out air in hose
5) Unscrew airline from tank and repack

The Air Bag: Manufacturing

The manufacturing process of the air bag's top plate consisted of five main parts; one for each main material. The main materials used were carbon fiber tubes, aluminum support brackets, Kevlar reinforcement sheets, pourable resin, and Rhino Liner rubber.

The first major step in the manufacturing process of the top plate was preparing the carbon fiber for the assembly. In order to do this the carbon fiber tubes had to be cut to fit the top of the bag. The tubes are 3.26” wide which means the top of the bag (24” diameter) could accommodate seven tubes side by side with a gap of approximately 1/16th of an inch between them to account for shifting during loading. The tubes were cut to approximate the diameter of the bag as shown in Figure 13**.**

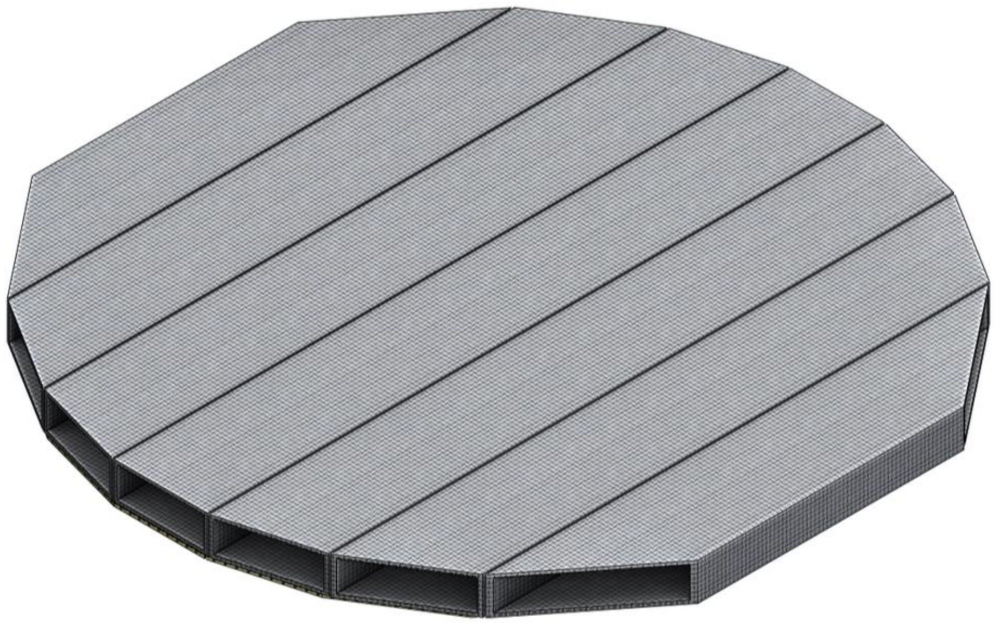

Figure 13 - Carbon Fiber Tubes Cut to Approximately Fit the Top of the Bag

Once the carbon fiber tubes were cut to the appropriate lengths, they then had to be drilled in order to allow the aluminum support brackets to be attached by rivets, as will be shown later.

The second major part of the manufacturing process of the top plate was preparing and attaching the aluminum support brackets. Two brackets were installed on each side of the carbon fiber plate. The 2” wide brackets were 1/16th of an inch thick and had to be cut to 22” in length so that they would not hang over the edges of the tubes or the bag. Cardboard shims were used during drilling to create a small gap between tubes to allow for a small amount of shifting during use, as seen in Figure 14. Once the brackets were cut and drilled they were installed on one side of the plate to keep it together properly during the next steps of the manufacturing process, as shown in Figure 15.

Figure 14 - Cardboard Spacers Were Installed During Drilling to Properly Space Drill Holes

Figure 15 - Carbon Fiber Top Plate With Aluminum Brackets on One Side

The next step of the manufacturing process of the top plate was pouring the resin. A custom resin was mixed and poured into each tube to increase its overall strength and durability and also to help prevent possible crushing. After a test pour in a scrap piece of carbon fiber it was discovered that the resin heated up too much during the curing process. To reduce the amount of mass of resin in contact and consequently reduce the heat generated during curing, a small piece 6”x2.75”x0.5” wood was inserted in the middle of the resin after it was poured in each tube (while it was still viscous) so that the heat would not compromise the strength and integrity of the carbon fiber. Also, this wood allowed the material to maintain a strong compressive strength. In order to decrease the amount of added weight from the resin it was decided that the resin would only be poured across the middle six inches of each tube and any concentrated or line load would be applied over the resin filled portion of the carbon fiber tubes perpendicular to the direction of the tubes-where they were the strongest. In order to make sure the resin was poured only in the midsection of each tube the plate was turned sideways and plugged from the bottom with wood pieces cut equally to length of 9” and the resin was poured in from the top. The pouring setup is shown in Figure 16**.**

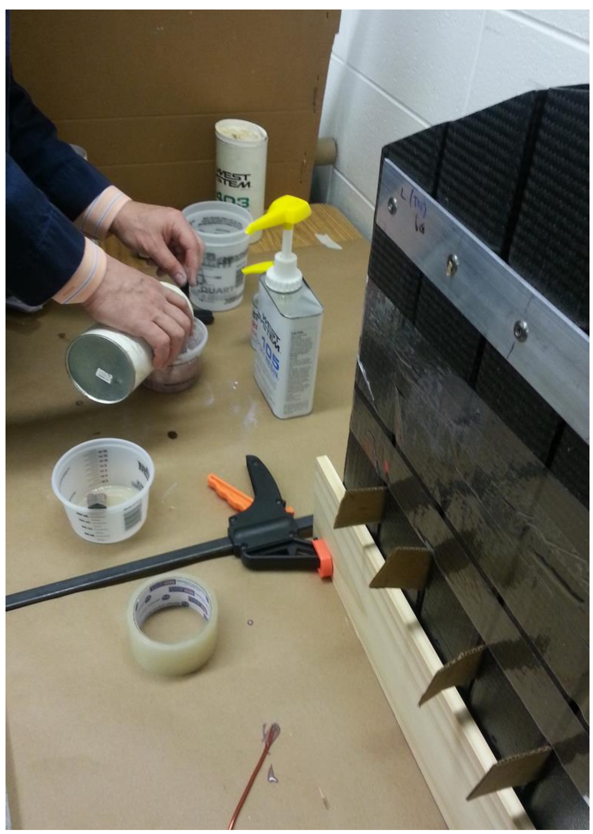

Figure 16 - Resin Pouring Setup

The next step after the resin cured and dried was to install the Kevlar reinforcement sheets and the other two aluminum support brackets on the bottom portion of the plate. Two Kevlar sheets were cut to fit the top plate and placed under the two remaining aluminum support brackets. The purpose of the Kevlar sheets was to add additional strength to resist the possible outward forces that may try to pull the plate apart. Also, the Kevlar will allow surface protection to the carbon fiber both while it is being carried and while in contact with the bag during use. The rivets were then first inserted through the aluminum, then through the Kevlar, and finally through the carbon fiber tube and riveted in place. Figure 17 shows the expanded view of the plate design.

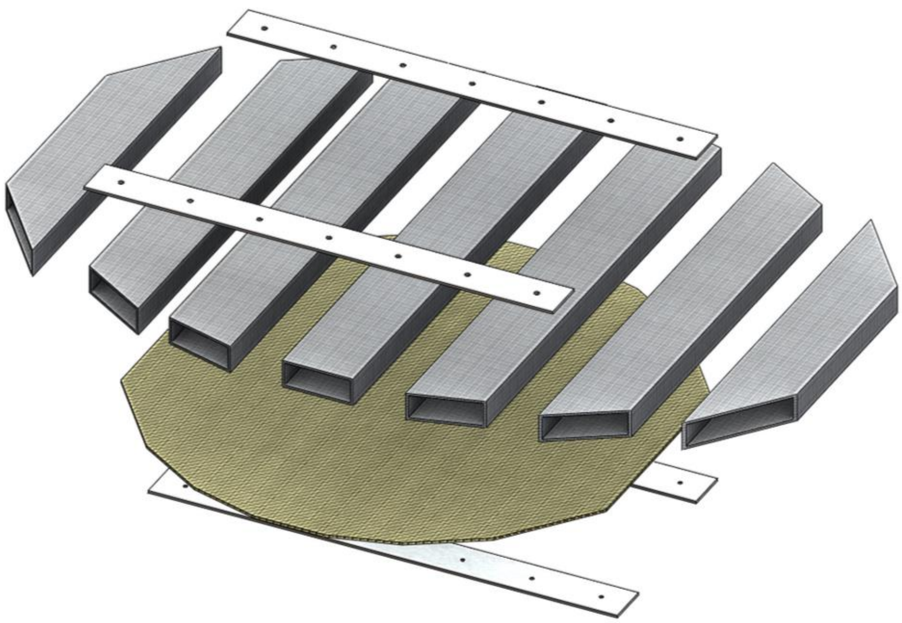

Figure 17 - Top Plate Expanded View

The final step of the manufacturing process for the top plate was to have the Rhino Lining rubber sprayed onto the top surface. This was done in order to increase the coefficient of friction between the load and the top plate itself to reduce the amount of slippage and also because it will offer protection to the surface of the carbon fiber itself. The completed top plate is shown in Figure 18**.**

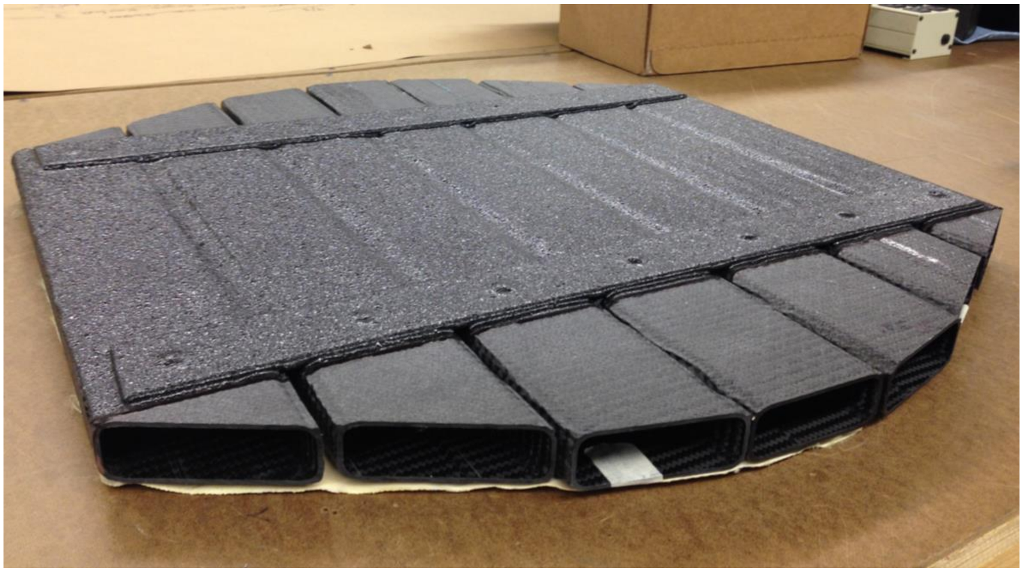

Figure 18 - Completed Top Plate

The Air Bag: Detailed Analysis

Weight

Due to the extreme design requirements associated with military rescue operations, the overall weight of the air bag solution comes in over the goal of 30 pounds. Having to lift 55000 pounds in a safe and controlled process required a robust design that focused on safety and effectiveness. To ensure the bag remains in place, a rubber mat was added along with stakes to be nailed into the ground. The top plate assembly was significantly strengthened to provide additional rigidity and grip. These additions considerably increased the weight of the design however were considered essential and therefore worth the extra weight. For possible weigh reductions in the future, lighter weight foam could be used in place of the solid resin inside the carbon fiber tubes. Also the ability to learn from full scale testing and seeing what works and what doesn't will allow for a better understanding of how each material performs and what can be modified or lightened. For the first run prototype used in this solution, the total weight comes out to be 53.1 pounds as seen below in Table 3.

Table 3 - Weights of Components

Component	Weight (lbs)
Air Bag	16.18
Top Plate	13.00
Air Tank	14.38
Air Line assembly	4.34
Rubber Mat	4.00
Stakes	1.00
Straps	0.20
Total	53.1

Determination of Required Lift Capacity

Although the vehicle being lifted can weight upwards of 50,000 pounds, analyzing a free body diagram shows that the required force to lift the vehicle can be much less than the 50,000 pounds of the vehicle. Figure 19 shows the vehicle on uneven ground with the force needed to lift and the weight of the vehicle straight up and down. Figure 20 is dimensioned to show how the required force was calculated to lift the vehicle.

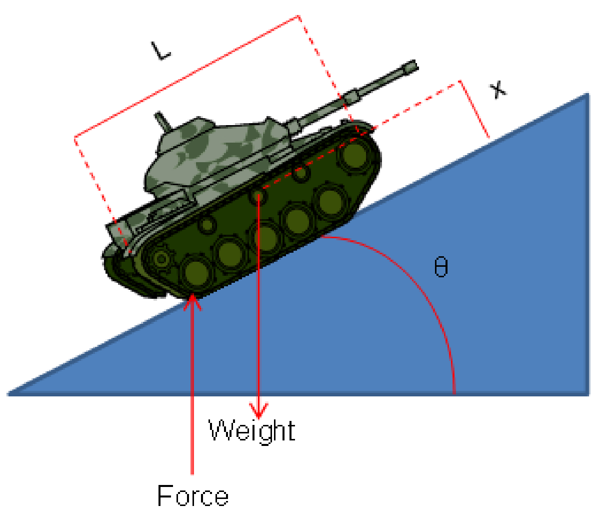

Figure 19 - Vehicle Free Body Diagram

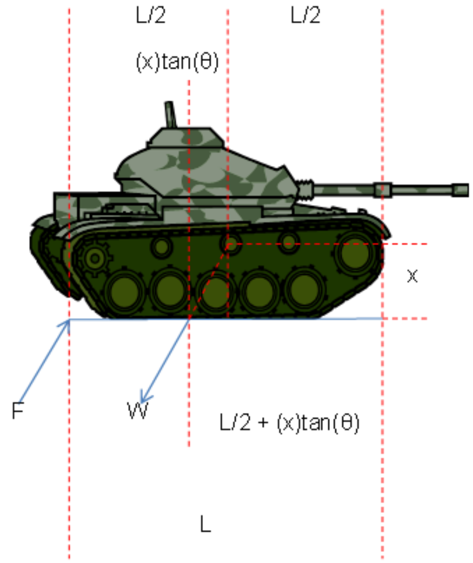

Figure 20 - Vehicle with Forces

$$\boldsymbol{F} = \frac{(\boldsymbol{W} * \cos(\boldsymbol{\theta})) * \left(\frac{L}{2} + \boldsymbol{x} * \tan(\boldsymbol{\theta})\right)}{\boldsymbol{L} * \cos(\boldsymbol{\theta})} \quad 1$$

F = Force required to lift vehicle

W = Weight of the vehicle

θ = Ground angle

L = Length of the vehicle

x = Height to center of gravity

Equation 1 is under the assumption that the center of gravity of the vehicle is in the dead middle of the vehicle front to back. This is the worst case scenario though; if the vehicle were heavily loaded on one side the lift would be performed on the opposite allowing for a smaller force to lift the weight. Under this assumption equation 1 can be used at any ground angle with any vehicle weight to determine the amount of force needed to actually perform a lift.

Bending & Shear Stress

To approximate the amount of bending stress experienced in the carbon fiber box beams, simple hand calculations were used to approximate the shear and bending moment. Simplified beam theory was used and followed the steps seen below in Figure 21. The Force acting along the center of the middle beam was found by dividing the weight of the vehicle by the number of box beams. A distributed load was applied to the bottom to represent the air bag pushing upwards to resist the weight of the vehicle. The shear and bending moment diagrams were then created to find the max moment to be F*L/8 where L is the length of the box beam (24 in).

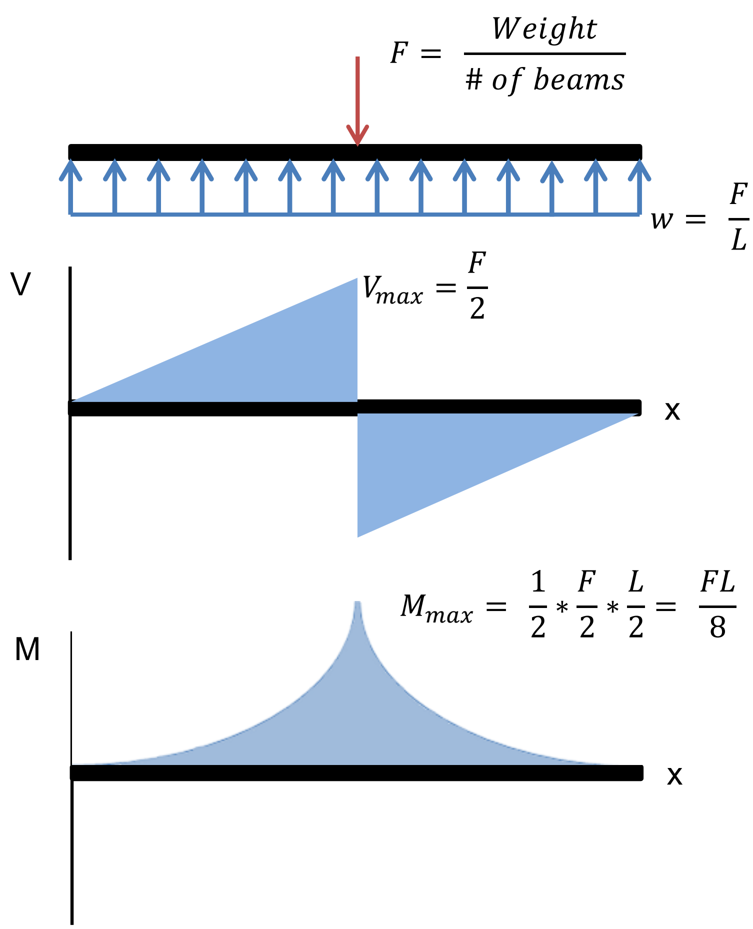

Figure 21 - Shear & Bending Moment Diagrams

With the max moment now determined, the bending stress can be calculated. First the moment of inertia across the neutral bending axis was determined using equation 2.

$$I = \frac{1}{12} * B * H^3 - \frac{1}{12} * b * h^3 \qquad 2$$

I = Moment of inertia

B = Outer base length

H = Outer Height

b = Inner base length

h = Inner Height

From here the bending stress was determined by equation 3.

$$\sigma_b = \frac{M * c}{I} \qquad 3$$

σ_b = Bending Stress

M = Max moment

c = Distance from neutral bending axis

I = Moment of Inertia

With these calculations, the max bending stress was determined to be 31,803 psi which is roughly a third of the bending strength of the carbon fiber beams. This rough approximation gives confidence that the beams will not fail at a safety factor of 3.

Pressure vs. Area

Pressure versus diameter analysis was done when designing the bag to determine the trade-off between bag size and required working pressure. The analysis was under the assumption that the entire top area of the bag is in contact with the load being lifted.

Figure 22 shows the pressure versus diameter trade-off graph for a bag that can lift 30,000 pounds.

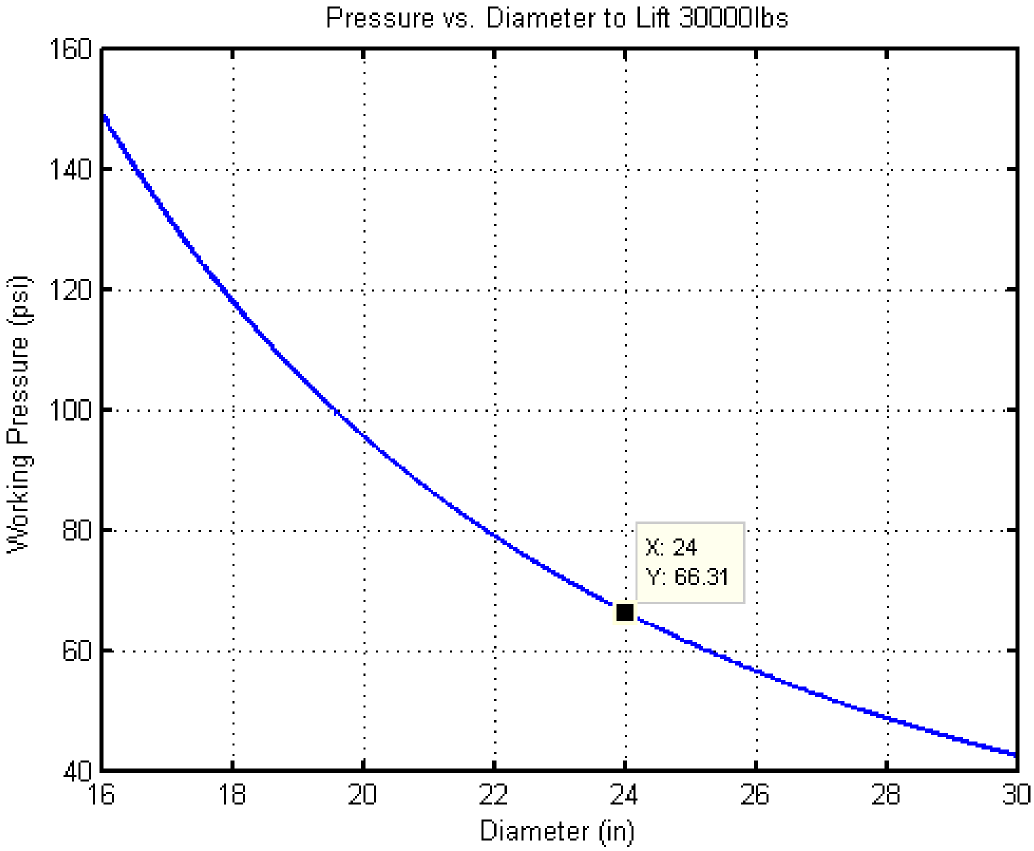

Figure 22 - Pressure vs. Diameter

$$P = \frac{F}{A} \tag{4}$$

$$A = \frac{\pi * d^2}{4} \tag{5}$$

P = Pressure

F = Force

A = Area

d = Diameter

Equations 4 and 5 show how Figure 22 was developed. Upon analyzing the graph, the team decided to choose a 24 inch diameter cylindrical bag because the required pressure to lift 30,000 pounds quickly rises when selecting under a 24 inch diameter while giving diminishing returns on the pack volume and weight.

ANSYS & Hoop Stress

SolidWorks was used to study the air bag stresses using finite element analysis. The FEA package in SolidWorks produced the Von Mises Stress contour plot as seen in Figure 23. The maximum stress of 5200 psi occurred around the center of the air bag, where expected.

The model was created using material properties of a nylon-laced rubber with a modulus of elasticity of 6000 psi and Poisson's ratio of 0.35. The air bag was modeled using shells with a thickness of 0.2 inches in standard orientation. Assuming the perfect loading conditions of the load being equally distributed over the top area, a pressure of 67 psi was applied to the top face. The bottom surface was considered to be simply supported on rollers and therefore zero displacement in the vertical axis was assumed.

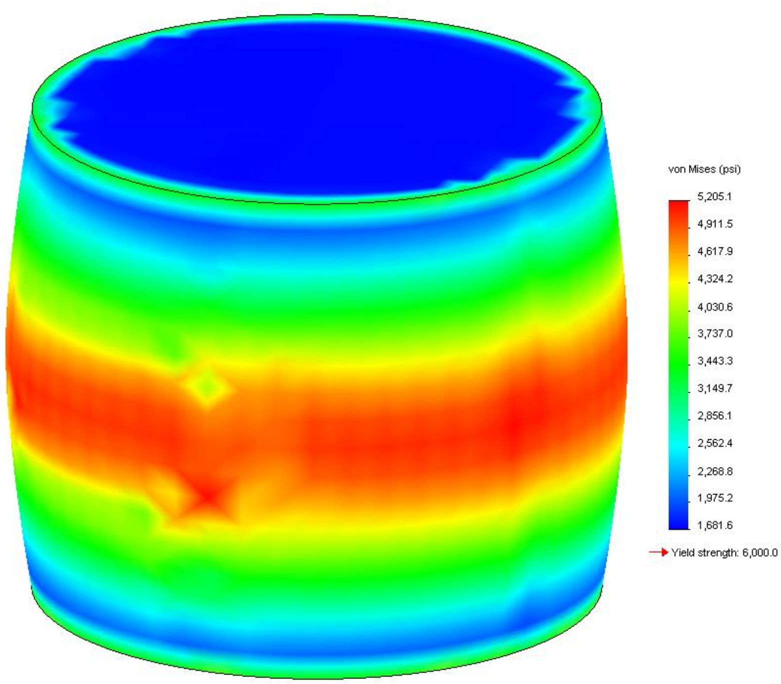

Figure 23 - FEA Results

To confirm the results from the FEA analysis, the air bag was considered as a thin-walled cylindrical pressure vessel and the hoop stress was calculated to be 4020 psi from the equation below.

$$\sigma_h = \frac{pd}{2t} \qquad 6$$

The calculated and simulated values are very similar and of the same magnitude. Therefore, there is confidence in our model and analysis.

Power Supply

To determine the required size of the air tank, the ideal gas law was used to compare pressures and volumes for initial and final conditions. At full inflation, the air bag has a volume of 10,857.34 in^3 at a pressure of 66.3 psi. The airlines were calculated to have a volume of 6 in^3 and an air cylinder has a volume of roughly 500 in^3. To determine how much air was needed, equation 7 below was used to compare the bag/line/tank assembly volume and pressure to atmospheric pressure. From this equation it was found that 29.7 cubic feet of compressed air would be needed to lift the vehicle.

$$V_{atm} = \frac{P_{assembly} * V_{assembly}}{P_{atm}} \qquad 7$$

Safety Precautions

Risk Analysis

In order to ensure safe operation of the air bag during testing the Ohio State AFRL Design Team conducted a risk analysis of the air bag, as required by the AFRL. The main concerns involved catastrophic failure of the air bag, including, over-inflation, loss of pressure, or rupture cause by projectiles. Specific counter measure will be taken in order to prevent injury and/or other damage. Perhaps the most imperative modification to the air bag will be the use of a relief valve that will not allow the bag to reach burst pressure, which could cause further injury or death. Equally as important is using a proper regulator that will ensure the air flows to the bag at the desired, controlled rate. The best line of defense to a fully ruptured bag is the use of adequate cribbing that will be applied continuously during the lift so that if the bag ruptures, the load will not be allowed to fall to the ground.

Another important concern that was addressed was the possibility of the air supply tank being ruptured either prior to or during use. If their air tank is ruptured prior to or during use, it could cause severe injury to those carrying, operating, or surrounding it. To prevent a rupture while packed, the air bag will be wrapped around the air tank, wince the multiple layers of Kevlar and rubber will provide adequate protection to the air tank from projectiles. Also, during use, those not directly using the device will stand outside of the blast radius when possible in order to minimize risk. If the air tank or air lines do get ruptured, the operators will carry a backup manual pump that can be used to inflate the bag and perform a rescue.

Stability is always a main concern. There is a risk that the load will shift or fall while being lifted. This could cause severe injury to those operating the device and/or those being rescued. In order to prevent further injury and damage, sufficient cribbing must be used at all times so that if the load becomes unstable during the lift, it will not fall onto anything or anyone except the cribbing. Another concern that was considered with stability is that of the bag slipping out from underneath the load. Similar to above, this could also lead to further injury and/or damage. This can easily be avoided by using a strong and durable rubber mat and stake combination to provide enough traction at the bottom of the bag to make sure the bottom stays in place during a lift. To make sure the top of the bag stays in place during lifting, the bag must be placed directly and evenly under the load that it is lifting in order to sufficiently distribute the load across the centermost portion of the bag to prevent tipping of the bag. If this is not possible the load could be lifted and then cribbed, and the bag could be slightly deflated and repositioned as the load shifts.

Two more, less dangerous, concerns were also addressed. The first minor concern is the airlines being ruptured. If the lines are ruptured during use the bag could slowly deflate, which could cause injury to anyone under the load. However, since this deflation would be very slow, since there would not be much air escaping the ruptured line, this problem could be solved simply by using efficient cribbing, as previously discussed. The rescue team will carry a backup manual pump (also as previously stated) in the event that the supply lines are ruptured, which will still enable them to perform a lift and therefore a rescue. The second more minor concern is that the stakes being used to secure the bottom of the bag slip out. If the bag is under a very heavy load the stakes could potentially fly out at a high velocity which could cause injury. This will be avoided through extensive stake testing in order to ensure the correct stakes are chosen and only used under appropriate conditions during use. Certain conditions (sand) may require no stakes at all for example.

Safe Lift Points

A safe lift point on the downed vehicle in crucial to the safety to the trapped and rescuing personal. The lift point can be found by estimating the center of gravity. By constructing mental lines from the side points of contact, through the center of gravity, and to the other side of the vehicle, the safe zone can be estimated.

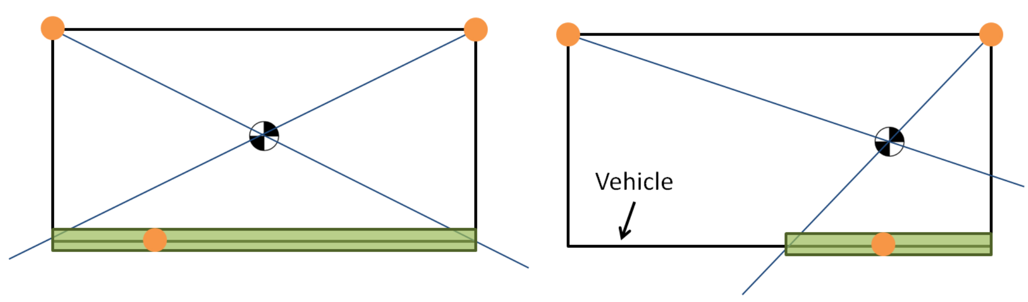

Figure 24 - Safe Lift Schematic

As long as the lift point is in the green “safe lift” zone (in Figure 24), the vehicle, aircraft, etc. will have three points of contact (orange) with ground ensuring that the vehicle will not become unstable during the lift.

Testing

Vehicle Lift Test

Once the air bag was ready to be used, multiple lifting scenarios were tested to gather as much information as possible about how the system works and what needs to be improved. A small pickup truck, a Jeep Cherokee, and a Cat V50D forklift were all lifted and are summarized below.

Truck

The first test performed with the air bag and a heavy load was conducted with a small pickup truck located in Ohio State’s Mechanical Engineering building. In this test, the air bag was situated under the frame rail of the truck, centered along the carbon fiber top plate as seen below in Figure 25. At this time, the carbon fiber top plate consisted of 7 box beams taped together with no additional support. As the bag inflated, it began lifting the truck as expected in a slow and controllable fashion. As the inflation continued and the vehicle began lifting off the ground, the plates began to slip off the frame rail and the whole bag tried to slip out. The box beams also started to separate from one another which was very problematic and uncontrollable. At this point the test was aborted and the bag was deflated. This test gave great new insight into the inflation process and made it clear what needed to be fixed. From this test it was determined that the carbon fiber tubes would need to have some sort of coating that would allow for much better grip with the vehicle. To account for this grip issue, the final top plate assembly was coated with the 3/16th inch Rhino Liner to provide a rough and durable contact point. It was also determined that the beams would need to be more rigidly attached to one another instead of using tape. Aluminum sheet metal strips were riveted to each box beam along with two layers of Kevlar to counter this problem. The Kevlar added additional strength when the beam try to stretch apart and the aluminum created a mechanical lock between each bar provided a significant in overall rigidity of the top plate assembly.

Figure 25 - Truck Lift Test

Jeep

The next test was performed outside on a grassy/muddy surface. In this test a Jeep Cherokee was lifted to see how the system operated in an outdoor environment without flat concrete surfaces as seen below in Figure 26. The bottom rubber mat was first placed on the ground in the approximate lifting location and then the air bag was placed on top of it. The top plate was then put in place and the lifting began. The first major observation from this test was the fact that the air bag doesn't inflate uniformly. One side of the bag tends to inflate first and this caused the top plate assembly to loose contact with the air bag. This issue was later addressed by covering the top of the bag and the bottom of the top plate assembly with high strength hook and loop (Velcro) material. The next key takeaway from this experiment was the fact that the bottom rubber mat should be permanently attached to the air bag to cut down on assembly time. The bag and mat had to be adjusted multiple times to get a nice alignment. Large Zip Ties were used to fix this problem and permanently attach the mat to the bag through the loops sewn onto the bag. The last realization made from this test was the fact that the top plate assembly should always be used unless there is a perfectly flat lifting surface on the vehicle being lifted. Without the use of the top plate, the load was unevenly distributed and the bag inflated by wrapping abound the structure and pushing horizontally instead of vertically on the load. This is extremely undesirable and significantly lowers the amount of weight that can be lifted by the air bag.

Figure 26 - Jeep Lift Test

Forklift

The final test was performed back in the Mechanical Engineering building on a 9000 pound Cat V50D forklift as seen below in Figure 27. The forklift was the heaviest vehicle tested and was the best representation of a full scale test. This lift tested the minimum compressible height of the system as well as the controllability of the lifting operation with the completed air-line assembly. The fork lift had a relatively small ground clearance and required the bag to be fully compressed. This tested the need to fully deflate and compress the bag on site and it was determined that the minimum achievable height was roughly 7 inches. Once the bag was in place, the lift sequence was initiated using the finalized air-line assembly. An adjustable pressure relief valve was added for lift control and safety and performed flawlessly. The easy to adjust valve allows for the bag to always remain in a safe operating pressure. When it comes time to lower the vehicle, the valve can be adjusted to act as an exhaust valve. This makes adjusting the lift height extremely easy and controllable. This final test gave the most realistic idea of how the full scale testing will go.

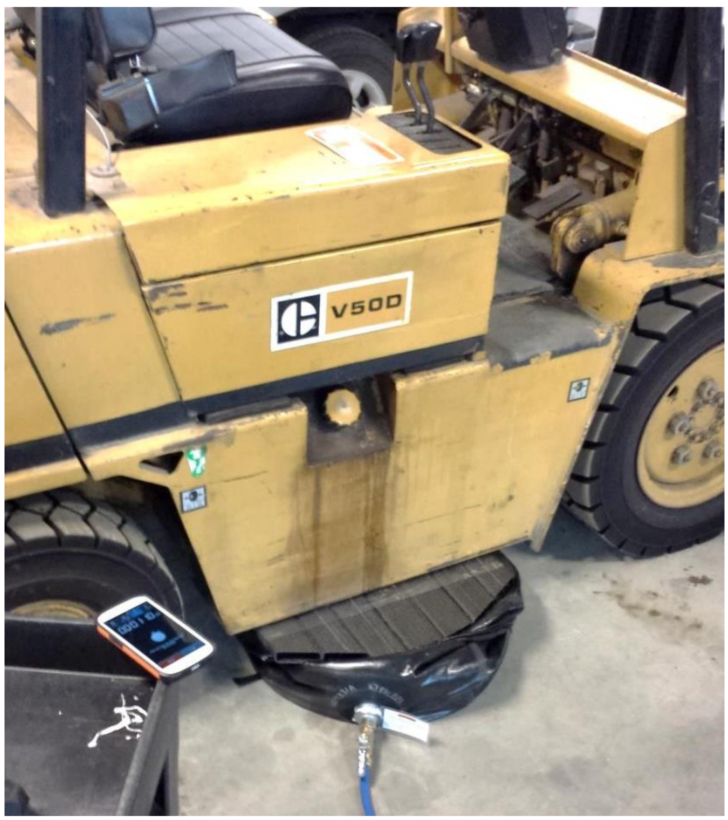

Figure 27 - Forklift Test

Carbon Fiber Crush Test

A crush test of the carbon fiber tubing used for the top plate, with the cross section depicted in Figure 28**,** was conducted to help determine its strength under loading.

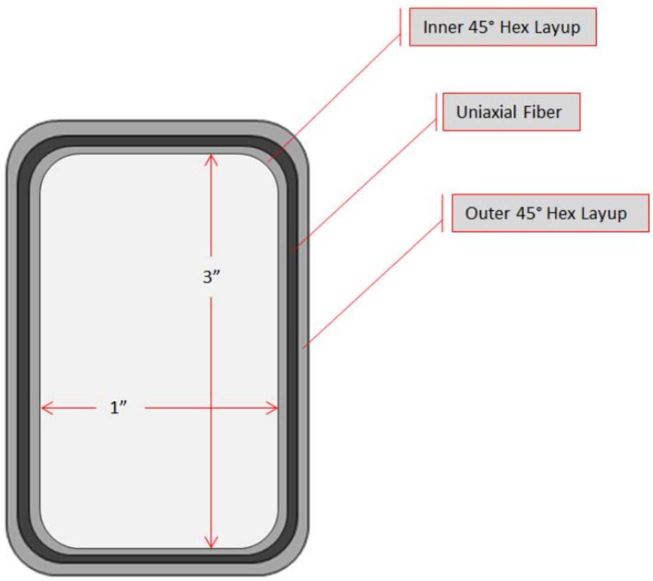

Figure 28 - Cross Sectional Box Area

A 5.25 inches long section was tested using an Instron machine. The load was applied along the centerline of the part, with the distance between fixed rollers being 3.125 inches. The setup is depicted in Figure 29 and Figure 30 before and after the test was conducted, respectively.

Figure 29 - Carbon Fiber Tube before Crush

Figure 30 - Carbon Fiber Tube after Crush

The tube tested experience failure at 2338 lb. The maximum moment generated at the midpoint by this force was 1826.5 in-lb, as equation 8 shows.

$$M_{max} = \frac{F_{max} * L_F}{2} \quad (8)$$

M_{max} = Maximum moment experienced by the part

F_{max} = Maximum force experience by the part

L_F = Distance from fixed roller to force (3.125 in./2 = 1.5625 in.)

A graphical representation of the results can be seen in Figure 31**.**

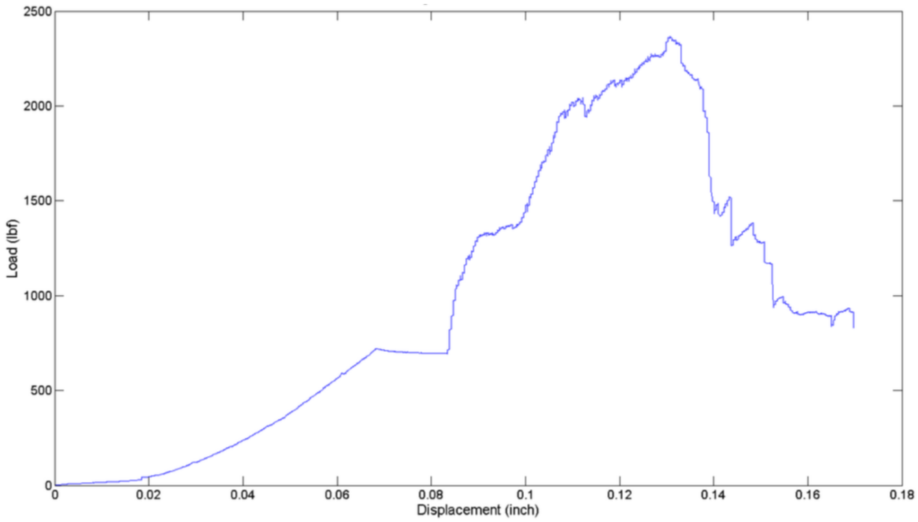

Figure 31 - Load Displacement Data for Carbon Fiber Crush Test

It was determined that the maximum force that each tube had to endure would be 4286 lb as equation 9 shows.

$$F_{tube\_max} = \frac{F_{tot}}{n_{tubes}} \quad 9$$

As the results of the test show, the carbon fiber tubes by themselves would not be able to withstand the same maximum force as the bag, so the resin was added. A crush test on a carbon fiber section filled with the pourable resin/wood combination was then tested using the Instron machine. The load was applied along the centerline of the part, with the same set up as the test without the epoxy, with the distance between fixed rollers being 3.125 inches. The setup is depicted in Figure 32 and Figure 33 before and after the test was conducted, respectively.

Figure 32 - Carbon Fiber Tube before Crush

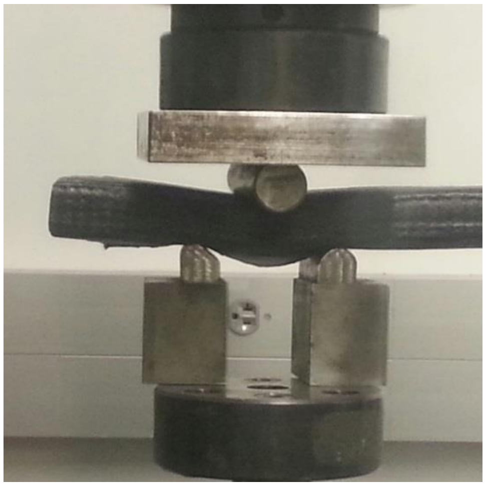

Figure 33 - Carbon Fiber Tube after Crush

The tube tested experience failure at 19,401 lbs which was over eight times the amount of force needed to crush the carbon fiber tube that was not filled with the resin/wood combination (2338 lb). The maximum moment generated at the midpoint by this force was 15,157 lb-in, as EQUATION 10 shows.

$$M_{max} = \frac{1}{2} * F_{max} * L_F \qquad 10$$

M_{max} = Maximum moment experienced by the part
F_{max} = Maximum force experienced by the part
L_F = Distance from fixed roller to force

The top plate consists of seven resin filled carbon fiber tubes which will more than support the maximum 30,000 lb lift capacity of the bag. As previously stated, at capacity, each tube would be expected to hold 4286 lb as Equation 10 shows, which is much less than the capacity of each tube. As a result, the top plate will not experience crushing under and loading conditions during the competition.

Stake Test

Initial Stake Comparison

A variety of stakes were analyzed in different terrains to determine the best overall option. A total of two corkscrew style ground anchors and four variants of common tent stakes were analyzed. Figure 34 shows the assortment of stakes considered.

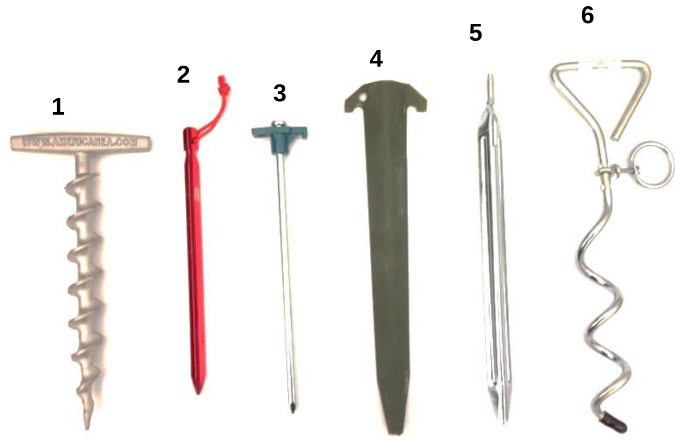

1	AEA Ground Penetrator
2	Coleman Tent Stake-
3	Coleman Std. Tent Stake
4	Standard Issue Military
5	Coleman Tent Stake-
6	Ground Anchor (Dog)

Figure 34 - Assortment of Stakes

Initially, each stake's weight and size were determined. Table 4 shows the most prominent dimensions and weight of each stake.

Table 4 - Stake Dimensions

	Weight (oz)	Height (in)	Width (in)	Ideal Packed Volume (4) (in^3)
AEA Ground Penetrator	5.7	9.5	4.5	128.25
Coleman Tent Stake- Flange	0.6	9	1	36
Coleman Std. Tent Stake	3.4	10	2	60
Standard Issue Military Tent Stake	3.7	12	2.75	33
Coleman Tent Stake- Blade	2.4	12	2	96
Ground Anchor	9.1	13	3.5	273

As seen in the table above, all of the stakes are relatively comparable in both size and weight. Since there are four loops and four tabs on the bottom of the air bag, the pack will be designed to hold 4 stakes. The corkscrew style ground anchors took up the most packed volume simply because they were the largest and widest. The standard military tent stakes took up the least amount of room due to their smaller size followed by the Coleman tent stake variants.

Stake Testing and Results

To compare the effectiveness of each stake, the pull out force was tested using a spring scale in both grass/dirt and compact sandy terrains. The tests were conducted by inserting each stake into the ground vertically and at 45 degrees, then gradually applying both a horizontal and vertical force separately. The testing apparatus and results are shown in Figure 35 and Figure 36 respectively.

Figure 35 - Testing Apparatus

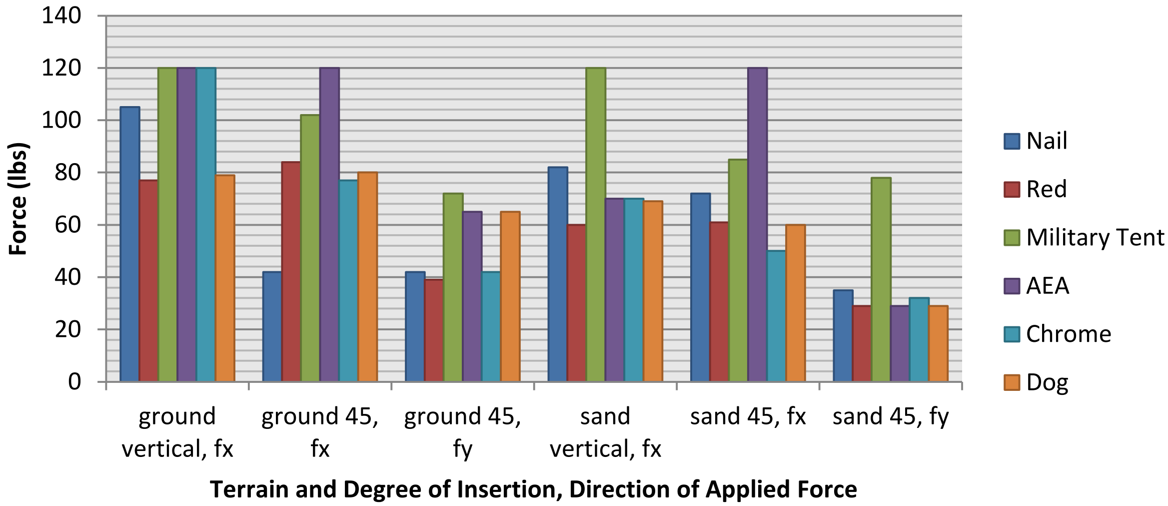

Figure 36 - Stake Comparison Test Results (Spring Scale Max at 120 lbs.)

Table 5 - Average Applied Force Causing Slippage

	Nail	Red	Military	AEA	Chrome	Dog
Avg. Force	63 lbs	58 lbs	96 lbs	87 lbs	65 lbs	64 lbs

From Figure 36, the red Coleman blade, chrome Coleman flange, nail and ground anchor (dog) performed the worst under the applied loads. The ground anchor did not work well in loose soil because it acted similar to an auger where it dug up a lot of the terrain. During the testing, the Coleman blade tent stake (chrome) plastically deformed at 120lbs, proving useless under heavy loads, shown in Figure 37. Thus, that stake was removed from further investigation.

Figure 37 - Plastically Deformed Stake

Clearly the two best stake options for all tests were between the AEA Ground Penetrator and standard issue military tent stake. The two are more closely analyzed in Figure 38.

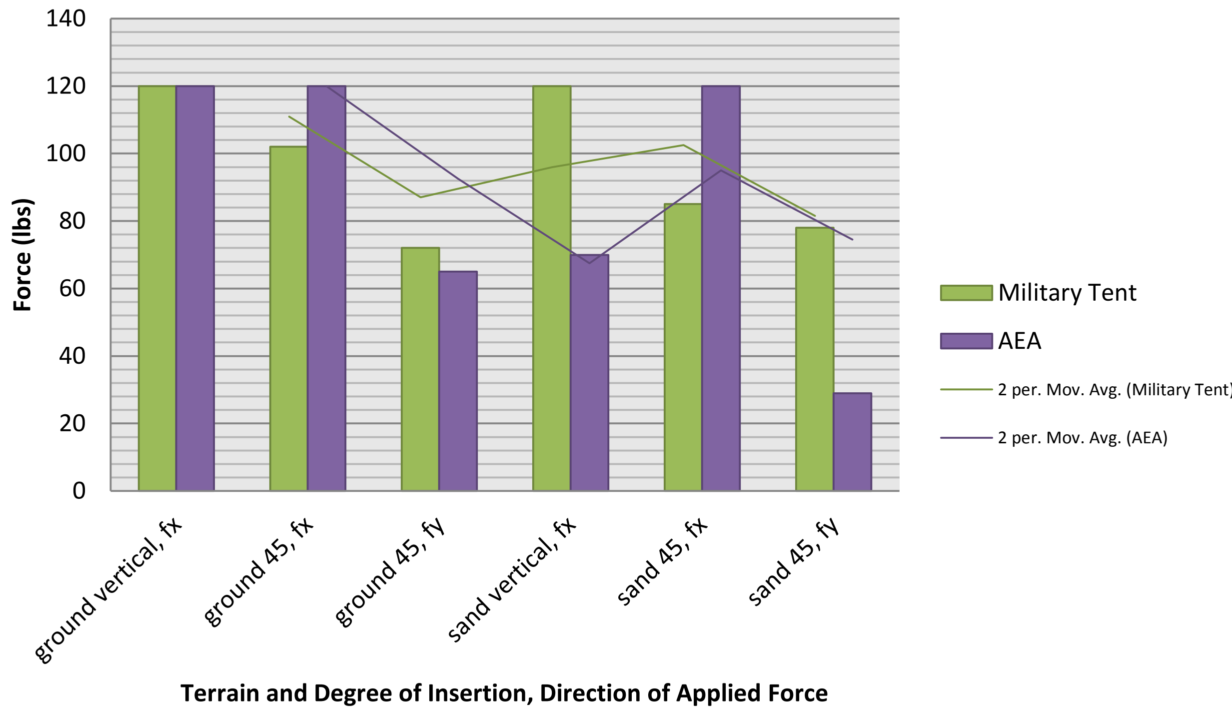

Figure 38 - Military Tent Stake vs. AEA Ground Penetrator

The width of the military tent stake forced more surface area against the ground to improve the vertical pull-out force in both terrains. The AEA Ground Penetrator maxed out the scale when inserted into the ground at a 45° angle and under a horizontal force for each terrain. The AEA Ground Penetrator also was able to be twisted into most terrains and tight spaces by hand due to the T-handle and screw shape; whereas, the traditional military tent stake required hammering in.

Dig Test

A potential set back in the team's overall performance is the time it takes to make clearance underneath the downed vehicle. Using a "standard issue" shovel, stopwatch, and wooden board, a test was conducted to estimate the time it would take to fit the kit into the necessary position.

Figure 39 - Dig Test Results

It took ~5 min to dig the hole seen in Figure 39 above. However, some of that time came from the poor quality of the shovel. The shovel bought at the local military store did not meet the expectations of what an actual, standard issue shovel. The collar that acts as the neck and allows the shovel to collapse was made of plastic. When a small torque was applied to the handle, the collar slipped out of the threads and caused the shovel to fail. A shorter dig time is expected in the actual competition.

Aspirator Test

In searching for a way to decrease time to inflate and decrease the amount of air needed in the compressed air tank, the idea of an aspirator arose. An aspirator is a

Venturi device or vacuum generator that can increase the volumetric flow rate of air that enters the air bag.

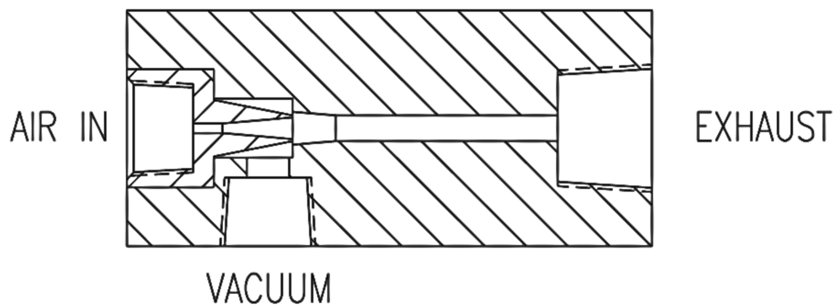

Figure 40 - Compressed Air Vacuum Generator

Venturi generators have been around for decades and are relatively simple to understand. As seen in Figure 40, air enters the device and travels through a converging-diverging nozzle. This creates a large pressure drop, less than atmospheric, which then creates the vacuum. Both flows meet and mix to exit the device and later entering the air bag.

To further understand the aspirator, many tests were executed. The first test was meant to become familiar with the operating conditions of the vacuum generator. The specs of the aspirator are listed in Table 6.

Table 6 - Vacuum Pump Specifications

Recommended Operating Pressure	70 psi
Maximum Vacuum	6.35 psi
Free Air	6.80 cfm
Air Consumption @ Op. Pressure	7.09 cfm

The set-up of this test, seen in Figure 41, included the device, two flow meters, a pressure gauge, a ball valve, and regulated shop air. Regulated shop air entered the Venturi vacuum at a controlled pressure. The flow rate of the vacuum was measured as well as the pressure at the exhaust side of the aspirator. The pressure here represented the pressure in the air bag and was controlled using the lever of the valve. The exit flow rate was also measured.

Figure 41 - Set-Up of Aspirator Testing

The exhaust and vacuum flow rates were directly affected by the inlet pressure. By increasing the inlet pressure, the vacuum flow rate increased, therefore increasing the exhaust flow rate. Results can be seen in Figure 42. Therefore, if the operating pressure was increased, the time to inflate the bag decreased.

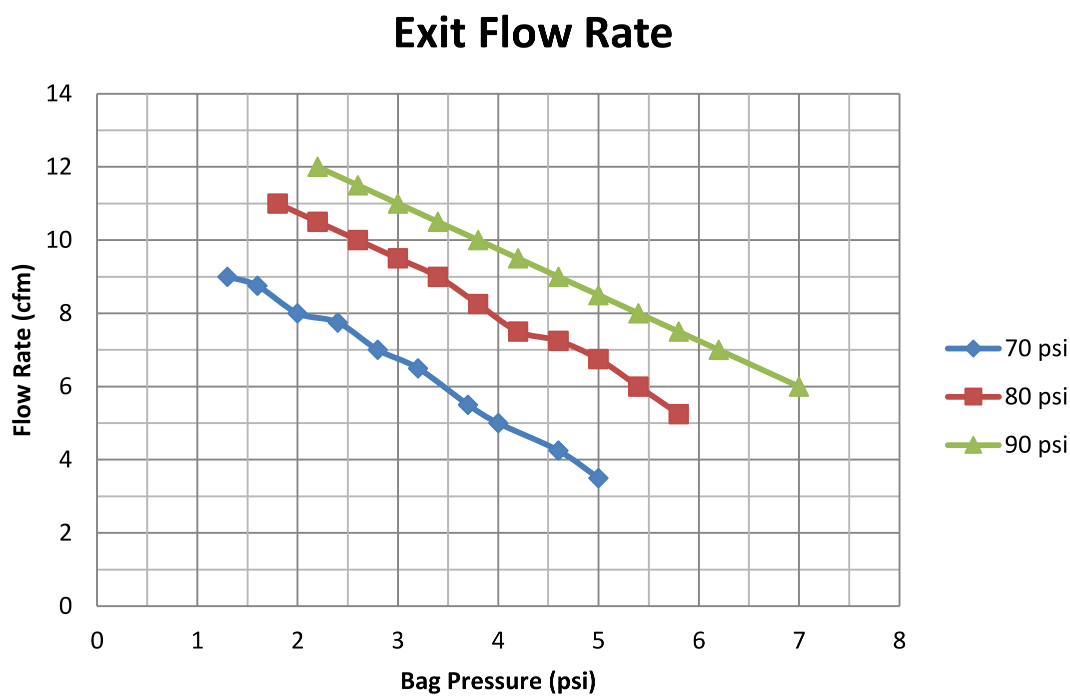

Figure 42 - Exhaust Flow Rate vs. Bag Pressure for Multiple Inlet Pressures

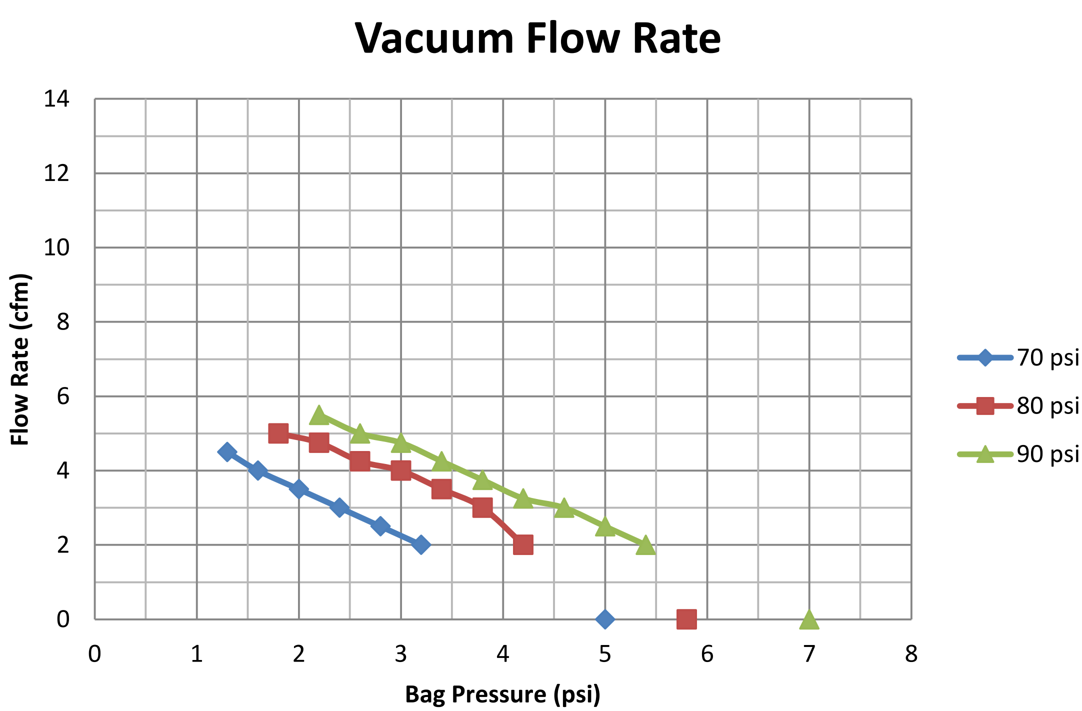

Figure 43 - Vacuum Flow Rate vs. Bag Pressure for Multiple Inlet Pressures

Above in Figure 43, the readings from the vacuum flow meter were plotted. The flow meters were unreadable below 2 cfm, resulting in the gap of measurements. As you can see, the result was confirmed; increasing the operating pressure allows for more “free air” to enter the air bag.

Using a piece of very thin and very light fabric, the point at which the air bag pressure overcame the device’s pressure drop (zero vacuum) was able to be plotted. When a vacuum is no longer being pulled, the aspirator becomes useless after the air bag reaches ~5 psi for an inlet pressure of 70 psi, close to the targeted bag pressure of 67 psi. A check valve at the vacuum is needed so that the inlet air will not escape through the vacuum port, wasting compressed air and not inflating the air bag.

Advantage of the Aspirator

A second set of testing was conducted to quantify the advantage of using a Venturi vacuum device. A small scale air bag was inflated using and not using an aspirator. The test set-up included the device, a pressure gauge, a ball valve, and regulated shop air. Regulated air entered the Venturi vacuum and exited the device in to air bag. The air bag was inflated to the same pressure over five iterations and the time to inflate was measured. The average times seen by multiple operating (inlet) pressures are tabulated in Table 7.

Table 7 - Average Time to Inflate Scaled Air Bag

Operating Pressure	No Aspirator	With Aspirator	Time Ratio
70 psi	13.584 sec	10.632 sec	0.783
80 psi	12.004 sec	8.808 sec	0.734
90 psi	10.620 sec	8.072 sec	0.760

Given the calculated time ratio, the aspirator decreases the inflation time by roughly 25% *until the air bag reaches 5 psi.*

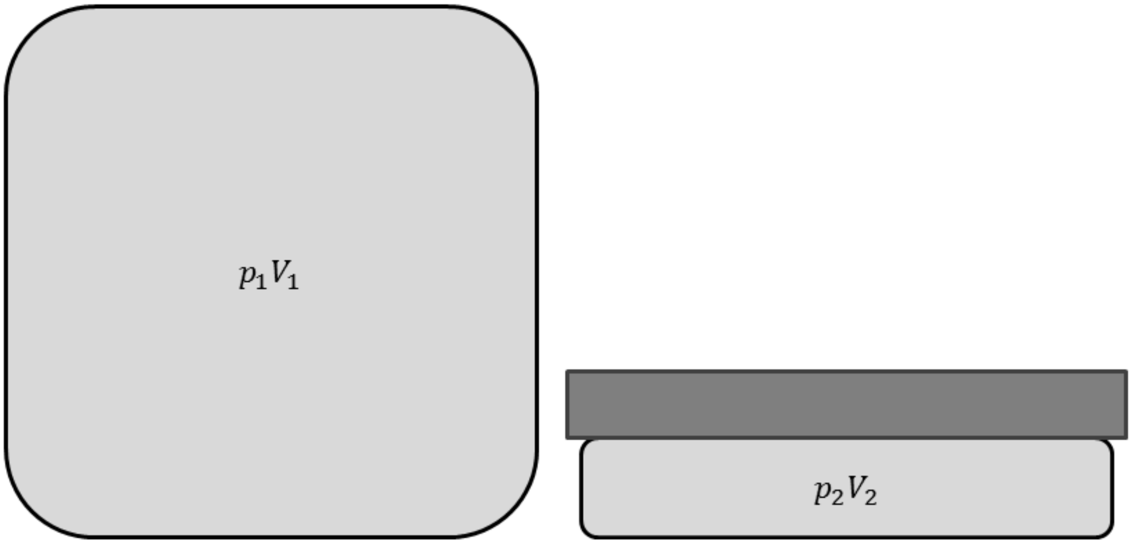

Figure 44 - Air Bag With and Without Load

Inflating the chosen air bag to 5 psi under no load took about 90 sec. However, when the air bag is under load, it does not need as much air to inflate to 5 psi because the volume is much less. This decreased the time to inflate dramatically.

Time to inflate is a function of the bag's pressure and volume. If the pressure of the bag is the same (5 psi) then the time to inflate is a function of volume. From Figure 44 it was assumed that because:

$$V_2 \ll V_1$$

Then:

$$t_2 \ll t_1$$

Since the aspirator is only useful up until the air bag reaches 5 psi, and it only saves 25% of the time, it is not worth the weight of the aspirator to include in the kit.

Summary

Pararescuemen execute unpredictable rescue and recovery operations as a part of their everyday routine. The air bag lift system detailed in this report accomplishes the major task of lifting a 55,000 lb vehicle 24 inches off the ground by tilting it up on one side. The air bag system provides a very robust yet simple design that is easy to set up and operate on site. Throughout the design process, safety and functionality remained the driving factors in determining what paths to take. With this in mind, some future improvements could possibly be implemented to further advance the system. To reduce overall weight, a lighter weight sprayable foam could be used to fill the carbon fiber box beams instead of the heavier resin. Additional research and load testing could then be performed to find the ideal foam that best balances strength and weight. Additional testing could also be performed under loads much closer to 55,000 lb to gain a better understanding of how each component reacts to extreme loading. Some other possibilities would include designing the system to be used in conjunction with the PJ Heavy RED kit. This kit includes a gasoline generator and many larger hand operated construction tools. These items could possibly be combined and modified to work with the air bag to create a safer and easier lift operation. The current design has what it takes to perform a successful rescue and recovery mission and with these proposed improvements has the possibility of being a very viable solution to the PJ's needs.

Appendix A – References

1. "Careers: Pararescue (Males Only)." U.S. Air Force. N.p., n.d. Web. 6 Apr 2014. <http://www.airforce.com/careers/detail/pararescue-males-only/>.

2. iQvalves, . "Venturi Vacuum Generators." Vacuum Sys Design Guide. N.p.. Web. 6 Apr 2014. <http://www.iqvalves.com/admin/productspdf/Vacuum Sys Design Guide.pdf>.

3. AXIOM Materials. "AX-5201M." *Structural Carbon Fiber Laminating Prepreg, 250F Cure*. 2011.

4. ACP Composites. "Mechanical Properties of Carbon Fiber Composite Materials." 2012. <http://www.acpsales.com/5-oz.-Aramid-Fabric-50-Wide-Plain-Weave.html>.

5. Petersen Products. " HOME CATALOG PIPE SPECS INSTRUCTIONS CASE STUDY CONTRACTORS CONTACT ABOUT 161-Series Medium Pressure High Lift Lifting Air Bags." 2011. <http://www.petersenproducts.com/161-0_MP_Lift_Bag.asp&xgt;.

Appendix B – Conceptual Designs

Below are depictions of some of the initial designs of the Ohio State AFRL team. The team developed over 40 different design ideas in many different categories (pneumatic, hydraulic, and mechanical).

Scissor Lift with Supporting Legs

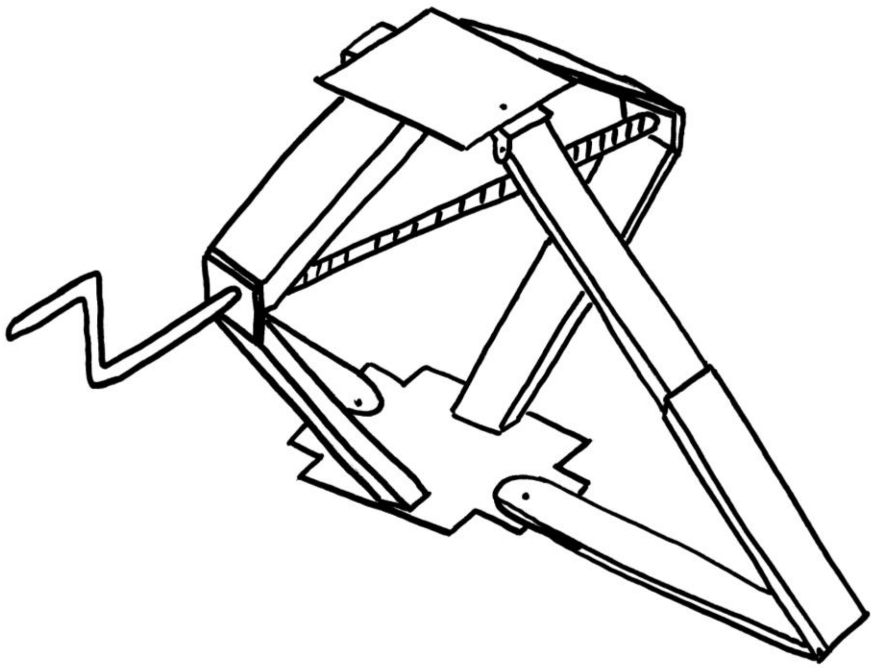

Iterative Air Bag Lifts with Scissor Supports

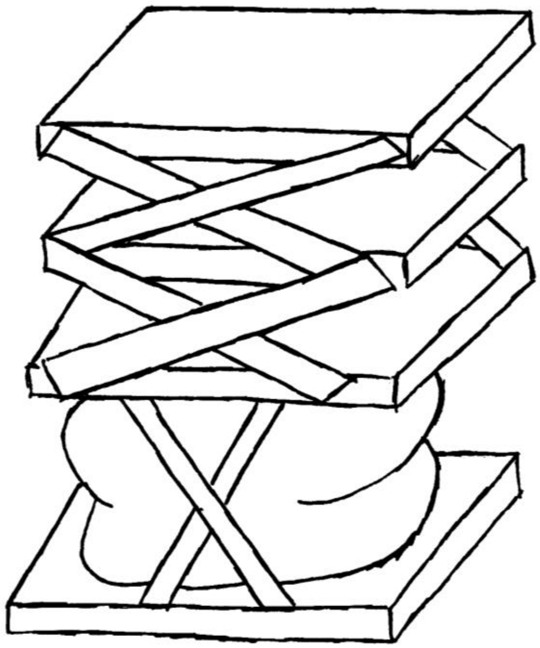

Air Bag with Collapsing Inner Support

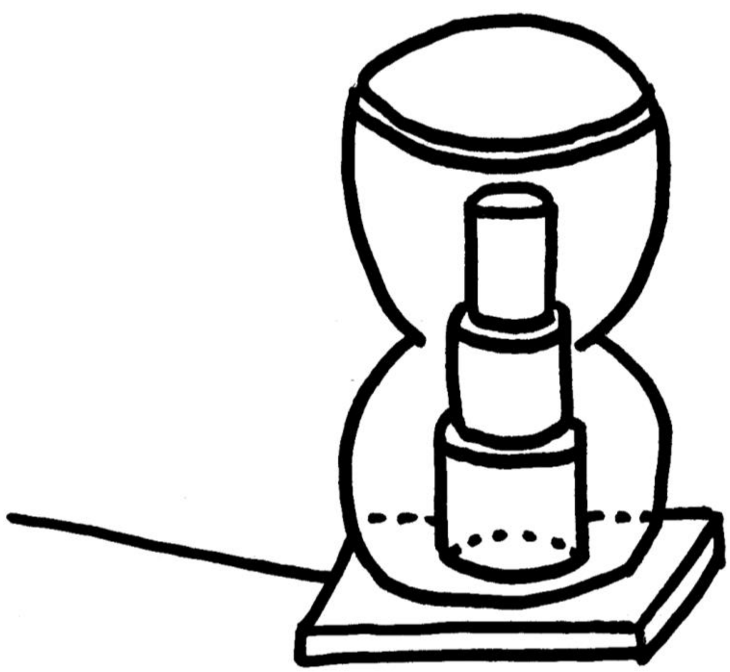

Hydraulic 4-Bar Linkage Lift

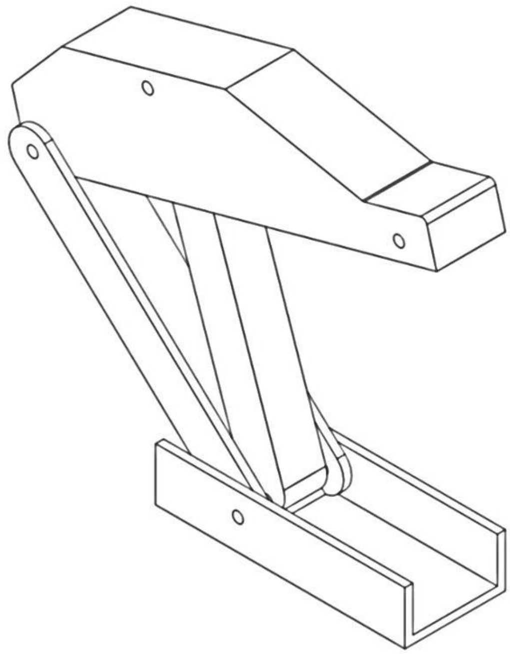

Toe Jack Utilizing Hydraulic Advantage

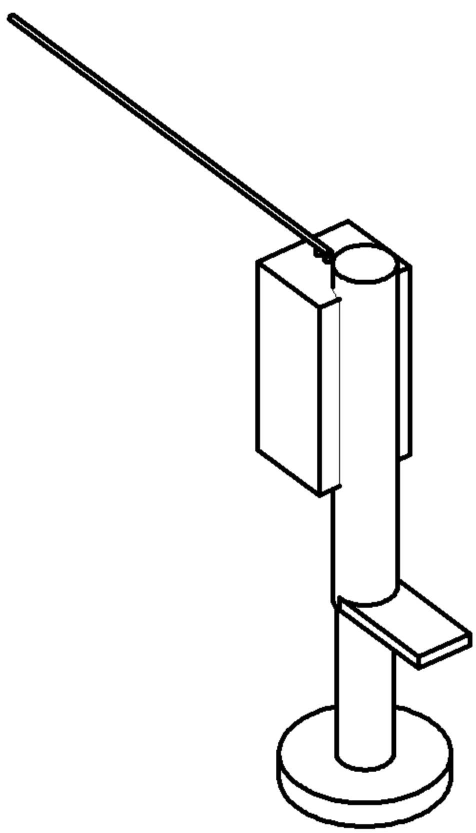

Appendix C - Carbon Fiber Tube Configuration

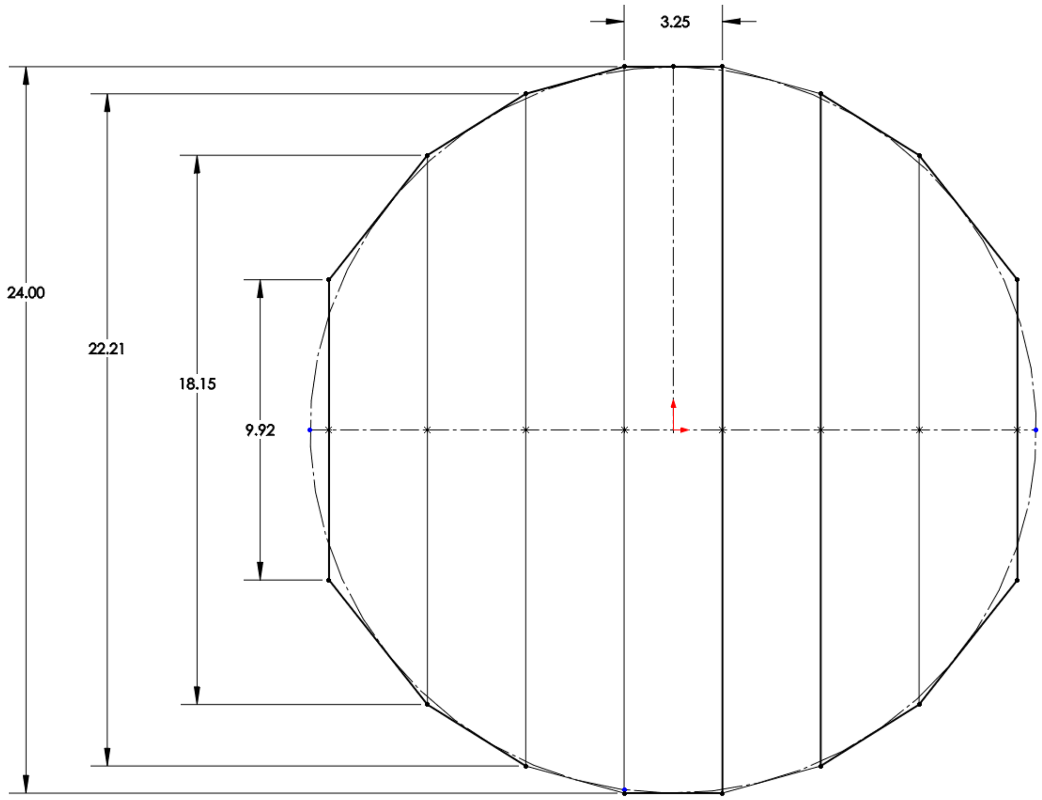

Appendix D – Sample Calculations

FBD Required Force to Lift

$$F = \frac{(W * \cos(\theta)) * \left(\frac{L}{2} + x * \tan(\theta)\right)}{L * \cos(\theta)}$$

$$= \frac{(45000\ lbs * \cos(20)) * (\frac{14.7\ ft}{2} + 5.15\ ft * \tan(20))}{14.7\ ft * \cos(20)} = 28238\ lbs$$

Pressure vs. Area

$$A = \frac{\pi * d^2}{4} = \frac{\pi * 24^2\ in}{4} = 452.39\ in^2$$

$$P = \frac{F}{A} = \frac{28238\ lbs}{452.39\ in^2} = 62.42\ psi$$

Max Moment

$$M_{max} = \frac{1}{2} * \frac{F}{2} * \frac{L}{2} = \frac{FL}{8} = \frac{4285.71 * 24}{8} = 12857.1 \quad in - lb$$

Moment of Inertia

$$I = \frac{1}{12} * B * H^3 - \frac{1}{12} * b * h^3 = \frac{1}{12} * 3.2 * 1.2^3 - \frac{1}{12} * 2.96 * .96^3 = .2426\ in^4$$

Bending Stress

$$\sigma_b = \frac{M * c}{I} = \frac{12857 * .6}{.2426} = 31803\ psi$$

Hoop Stress

$$\sigma_h = \frac{pd}{2t} = \frac{(67\ psi)(24\ in)}{2(0.2\ in)} = 4020\ psi$$

Air Tank Volume

$$V_{atm} = \frac{P_{assembly} * V_{assembly}}{P_{atm}} = \frac{66.3\ psi * 11363.3\ in^3}{14.7\ psi} = 51560\ in^3 = 29.7\ ft^3$$

Crush Test

$$M_{max} = \frac{F_{max} * L_F}{2} = \frac{2338\ lb * 1.5625\ in}{2} = 1826.5\ in - lb$$

$$F_{tube\_max} = \frac{F_{tot}}{n_{tubes}} = \frac{30000lb}{7\ tubes} = 4286lb/tube$$

$$M_{max} = \frac{1}{2} * F_{max} * L_F = \frac{1}{2} * 19401lb * 1.5625in = 15157lb - in$$

Appendix E – Excel Spreadsheets

Determining Number of Box Beams:

Box Beams										
# rods	Height (in)	Width (in)	Thickness (in)	Force (lb)	Area (in^2)	Inertia (in^4)	Moment (in-lb)	Bend Stress (psi)	Shear Stress (psi)	Fail???
5	1.2	3.2	0.12	6000	0.998	0.2426	18000	44524	6010	Yes
6	1.2	3.2	0.12	5000	0.998	0.2426	15000	37103	5008	No
7	1.2	3.2	0.12	4286	0.998	0.2426	12857	31803	4293	No
8	1.2	3.2	0.12	3750	0.998	0.2426	11250	27828	3756	No
7	1.2	3.2	0.12	4286	0.998	0.2426	12857	31803	4293	No

Air Tank Calculations:

	Diameter	Area (in^2)	Volume (in^3)	Pressure (psi)	Volume tank needed (in^3)
Bag 1	20.00	314.16	7539.82	95.49	160.00
Bag 2	24.00	452.39	10857.34	66.31	160.00
Bag 3	36.00	1017.88	24429.00	29.47	160.00
Air lines			11.78		

Weight Determination:Error! Not a valid link.

Aspirator Testing:

Operating Pressure (psi)	Back Pressure (psi)	Vacuum Flow (cfm)	Exit Flow (cfm)
70	1.3	4.5	9
70	1.6	4	8.75
70	2	3.5	8
70	2.4	3	7.75
70	2.8	2.5	7
70	3.2	2	6.5
70	3.7		5.5
70	4		5
70	4.6		4.25

70	5	0	3.5
Operating Pressure (psi)	**Back Pressure (psi)**	**Vacuum Flow (cfm)**	**Exit Flow (cfm)**
80	1.8	5	11
80	2.2	4.75	10.5
80	2.6	4.25	10
80	3	4	9.5
80	3.4	3.5	9
80	3.8	3	8.25
80	4.2	2	7.5
80	4.6		7.25
80	5		6.75
80	5.4		6
80	5.8	0	5.25
Operating Pressure (psi)	**Back Pressure (psi)**	**Vacuum Flow (cfm)**	**Exit Flow (cfm)**
90	2.2	5.5	12
90	2.6	5	11.5
90	3	4.75	11
90	3.4	4.25	10.5
90	3.8	3.75	10
90	4.2	3.25	9.5
90	4.6	3	9
90	5	2.5	8.5
90	5.4	2	8
90	5.8		7.5
90	6.2		7
90	7	0	6

Stake Testing:

	ground vertical, fx	ground 45, fx	ground 45, fy	sand vertical, fx	sand 45, fx	sand 45, fy	Average Force
Nail	105 lb	42 lb	42 lb	82 lb	72 lb	35 lb	63 lb
Red	77 lb	84 lb	39 lb	60 lb	61 lb	29 lb	58 lb
Military Tent	120 lb	102 lb	72 lb	120 lb	85 lb	78 lb	96 lb
AEA	120 lb	120 lb	65 lb	70 lb	120 lb	29 lb	87 lb
Chrome	120 lb	77 lb	42 lb	70 lb	50 lb	32 lb	65 lb
Dog	79 lb	80 lb	65 lb	69 lb	60 lb	29 lb	64 lb

Appendix F – MATLAB Files

```
% Air Bag Limitations
% AFRL Research Project

clear
clc

S_H=6000; %psi

%% Thin Wall Approximation
d=16:.01:30; %in

for i=1:5
    for j=1:length(d)
    t(i)=i/5;
    p_thin(i,j)=S_H*2.*t(i)./d(j);
    A(j)=pi/4*d(j).^2;
    end
end

figure(1)
plot(A,p_thin(1,:),A,p_thin(2,:),A,p_thin(3,:), ...
     A,p_thin(4,:),A,p_thin(5,:))
title('Pressure vs. Area (Thin-Walled Approximation)')
xlabel('Area (in^2)')
ylabel('Working Pressure (psi)')
legend('t=0.2"','t=0.4"','t=0.6"','t=0.8"','t=1"')
```

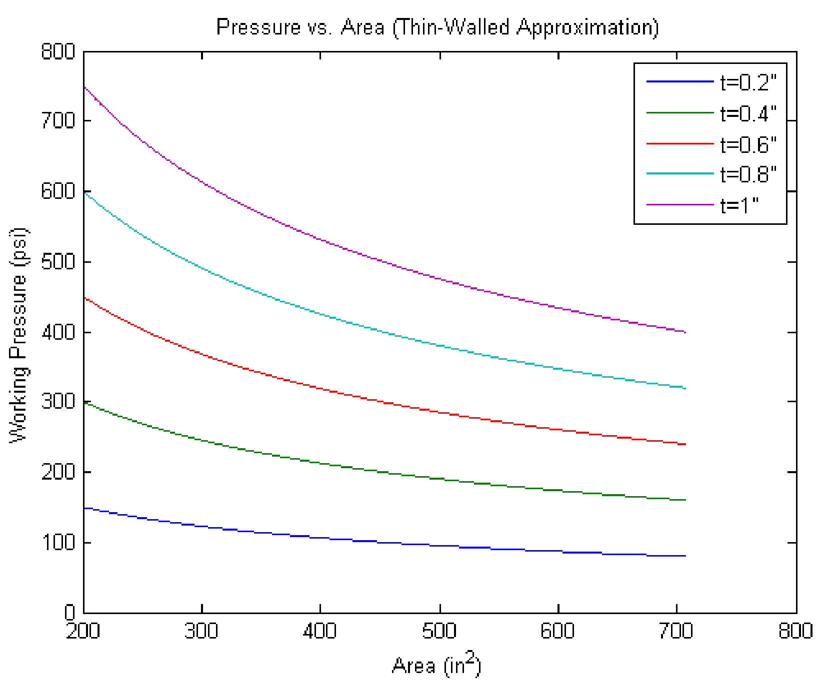

2013 Ohio State University AFRL Design Challenge

Presented on 4/16/13

Students:

Aaron Gearhart   Rachel Hudson   Devin Krause   Emily Sheets

John Tholen   Bill Tolbert   Ross Turek

GTA:

Ilia Gotlib

Advisor:

Dr. Anthony Luscher

Table of Contents

Abstract

Battlefield Airmen depend on their equipment for their safety and the success of their missions. During rescue and assault operations, airmen have experienced difficulty traversing irrigation canals, moving from rooftop to rooftop, and crossing minefields, unstable structures, and compound walls. To face these obstacles with ease, ground forces need a lightweight, portable, device that could function as either a ladder or a bridge. Before all else, Master Sergeant Bean provided insight of the airmen's wants and needs. Subsequently, the design focus for the bridge became the packing volume and assembly speed. Multiple conceptual designs were considered, analyzed, and rapid prototyped to arrive at a final concept and design. Various material combinations were considered throughout the design iterations. Carbon fiber box sections and aluminum connection elements were used to create the final structure. The unique joints allow each element to be universal and symmetrical and add versatility in utilization.

Testing and analysis is an essential step in the product development process to provide certainty to the customers. Customers want to know that the final product works under pre-specified conditions. The final design has been subject to a variety of experiments to assess its reliability, dependability and stability in compliance with the airmen's needs. After analysis, the resulting device weighs 54 pounds, spans 12 feet, and fits into slightly more than a 1 cubic foot rucksack. The bridge provides Battlefield Airmen with a device that successfully and safely assists in their missions.

Introduction

The contents of a Battlefield Airmen's rucksack often are the constituents warranting a safe return. The Ohio State Bridge provides a solution to serve as a dual ladder and bridge function that is highly compatible and versatile. The device's main features are the volume and load capacity objectives. The device span is considerably compromised, which is a tradeoff associated with the concentration on the volume requirement. In tandem to the volume focus, efforts were geared toward confirming the device was fully capable of withstanding a load of 350 pounds. The overall weight of the device is more than desired, which gives opportunity for continuous improvement efforts upon completion of the university challenge.

The User: Battlefield Airmen

Battlefield Airmen are a special operations force of the Air Force that performs unique ground operations essential to control, enable, and execute in the air. These include Combat Controllers, Para-Rescuemen, Tactical Air Control Party members and Special Operation Weather Technicians [1]. Special Tactics Battlefield Airmen have globally experienced adversity in navigating across various obstacles during rescue and assault operations. These obstacles include but are not limited to fast flowing streams, crevasses, rock formations, minefields, one rooftop to another and/or unstable structures. The current solution in facing these obstacles is an aluminum ladder.

Figure 1: Airmen face various terrains and obstacles on missions.

The User's Needs

Issues with the current solution are its bulkiness, its weight, and its incompatibility with the use of Night Vision Goggles (NVGs). When the airmen are wearing the NVGs, their depth perception is compromised [2]. An ideal device would be lightweight, portable, and possesses multiple purposes. Master Sergeant Bean was the source used to gain additional insight of the wants and needs of airmen.

Master Sergeant Bean's main concern was the packing volume, followed by the load capacity of the bridge. The weight of the bridge was not as pressing for the competition due to the wide variety of material options that exist and are currently being researched and tested by the military. The OSU team created an easy-to-assemble modular design. Being modular would be advantageous for the case where more than one airman would participate in the assembly process. Another advantage of a modular bridge arises when facing different obstacles. Pre-mission intelligence may list explicate obstacles ahead of time and warn the airmen what they will be facing. The need for quick assembly pertains to the safety of the airmen. If an airmen team is under fire, a fast assembly is crucial.

Master Sergeant Bean's also suggested that the bridge to be quiet. If the airmen are executing an operation that requires stealth, the bridge, as a whole, needs to be inaudible to avoid discovery by the enemy. When the bridge is being assembled, used, and disassembled, it should not produce a noise level that will jeopardize their position. To piggyback on ensuring the airmen's position is not jeopardized, careful lighting needs substantial consideration. The OSU team decided that lighting would be helpful to make certain the airmen are stepping on the rungs, but at the same time avoid ceasing their position. Therefore, an enable-all switch lighting feature was advised to give the airmen the option to turn the lighting on at their own discretion.

Master Sergeant Bean also stressed that the bridge be compatible to personnel recovery operations. The Air Force Pararescuers (PJs) are skilled in treating injuries and bringing people out of difficult situations day or night [3]. When considering personnel recovery, the width of the bridge needs to be compatible with the width of a Skedco. The lighting feature would provide assistance to PJs during personnel recovery. Master Sergeant Bean also recommended the bridge itself be capable of being used as a gurney.

Figure 2: Pararescuemen face obstacles they must negotiate while carrying injured men. Providing a bridge adaptable to Skedcos was a driving component during the design process. (WPAFB Museum display)

Master Sergeant Bean emphasized the trust that airmen put in the equipment they use in the field. To instill trust in the airmen when using the bridge, various features are needed. A quick, quiet assembly, proper lighting, and stability are imperative for gaining the airmen's trust. The OSU team decided to create an end piece that would provide substantial gripping to various surfaces, such as mud, sand, aluminum roofs, and gravel. The Special Operations Weather Technicians (SOWT) assess and interpret weather and environmental intelligence and assist in the mission planning [4]. Before embarking on an operation, the SOWT provides needed information that tells the airmen what conditions the bridge will be under. Therefore, the airmen would know ahead of time which end piece to take on the mission.

Goals of the Bridge

Table 1: Goals that drove the design process

Goal	How the goal drove the design
Packing Volume	All conceptual designs were based on fitting the bridge into a 12" x 24" x 6" rectangular prism.
Single, Uniform Element	The design would not have separate rungs and rails, but use a common element that could be used as either, therefore allowing a simple assembly.
Full Symmetry	The orientation of the single element would not be a concern for the airmen, as both ends are the same, permitting an easier assembly.
Robust Bridge	The rough conditions airmen encounter demand a bridge that has great strength and durability.

The Bridge: Overview

The Ohio State Bridge consists of 24 uniform elements, which together weigh approximately 54 pounds. The packaged volume of the device is ____, almost one cubic foot. The total length of all assembled elements is 13.5 feet, shown in Figure 5. The total span length is 12.0 feet with 9 inches on both ends to provide support. The composition of a single element consists of hollow carbon fiber rectangular tube with a reinforced slot through the middle and 6061 Aluminum end joints. The single element is shown in Figure 3. Figures 4 and 5 show the bridge assembled.

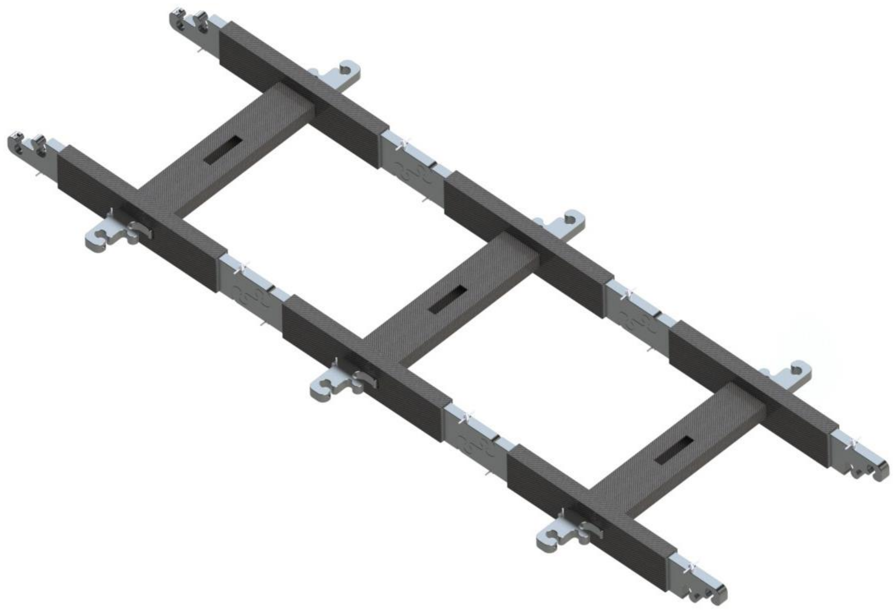

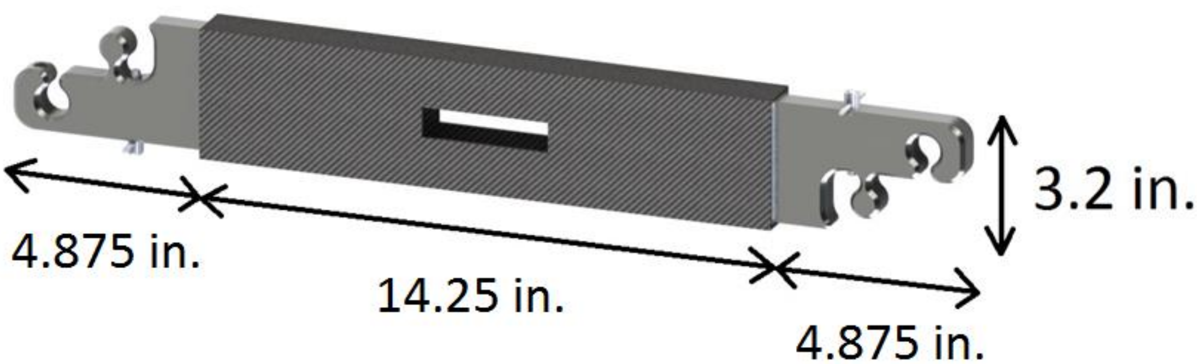

3.2 in.
4.875 in.
14.25 in.
4.875 in.

Figure 4: Close View of Assembled Bridge

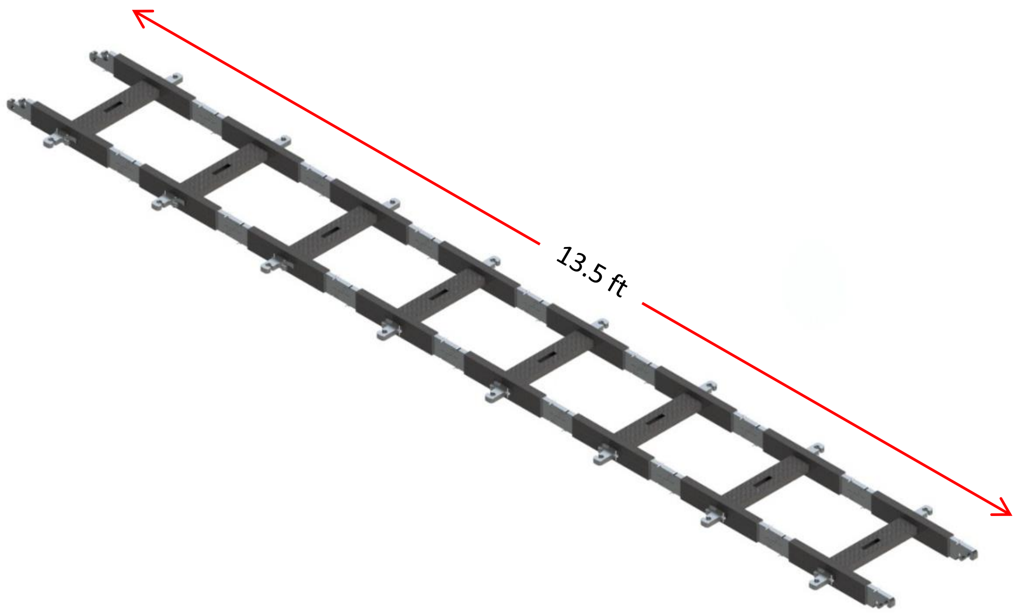

Figure 5: Fully Assembled Bridge Spanning 13.5 ft

The
Bridge: Features & Components

Carbon Fiber Tubes

Wolf Composites supplied the carbon fiber box sections (see Figure 6). The box sections are robust, created with a unidirectional fiber layer with a wrap to give a wall thickness of 0.125 inches. The tubes are box sections with inner dimensions of 3” x 1” and the tubes were cut into sections 14.25 inches in length.

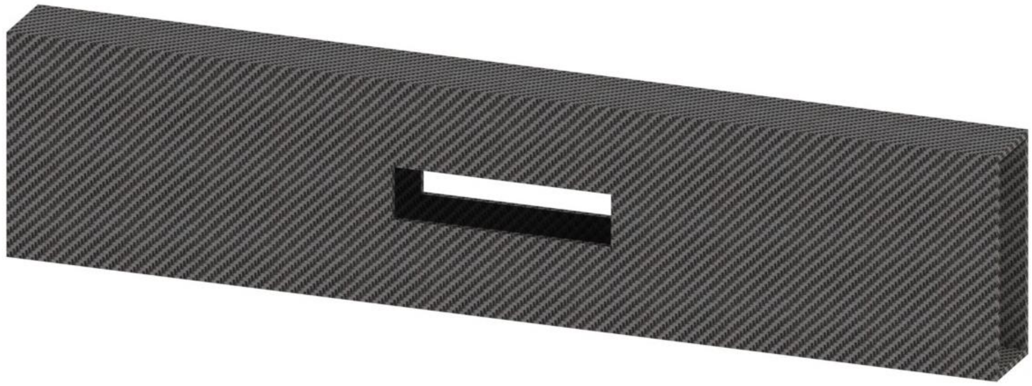

Figure 6: Carbon Fiber Tube

This was the aspect of design with the largest engineering trade off. The larger and thicker the cross-section of the tube the greater the strength, but negatively it would increase the weight and, more importantly, the packing size. An in-depth study considering all worst case scenarios of loading in both the vertical and horizontal deployment, buckling, both overall and local, and maximum deflections was performed in order to determine the optimal cross section for minimizing weight and packing volume and maximizing strength. An excel spreadsheet was created that compared different variations of base, height, and thickness measurements. Table 2 gives the considered dimensions of these measurements. Every possible combination of base, height, and thickness was examined in the spreadsheet. When comparing all the results and considering supply limitations, it was concluded that a 3.25” x 1.25” box section would best suit the needs of the Air Force. Table 3 shows a few variations from the spreadsheet. The Custom variation was the decided dimensions. The entire Excel spreadsheet may be found in the Calculations Appendix at the end of this document.

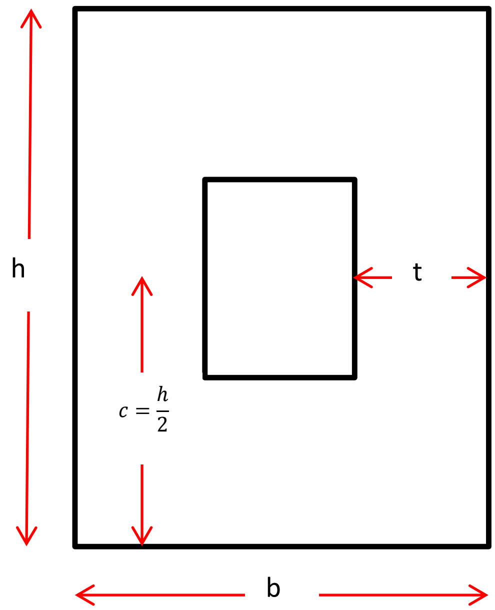

Figure 7: Rectangular Tube Cross-Section

Table 2: Base, Height, & Thickness Variations used in Excel

Dimension	1	2	3	4	5	6	7	8	9
b	1.000	1.250	1.500	1.750	2.000	-	-	-	-
h	1.000	1.250	1.500	1.750	2.000	2.250	2.500	2.750	3.000
t	0.075	0.100	0.125	-	-	-	-	-	-

Table 3: Yield Determinacy of Various Variations (Yielding occurs at 60,000psi)

Variation	b (in)	h (in)	t (in)	c (in)	Iy (in^4)	Ix (in^4)	20 ft Stress (psi)	Does it Yield (20 ft)
Custom	1.250	3.250	0.125	1.625	0.279	1.326	25738	No
1	1.000	1.000	0.075	0.500	0.040	0.040	263602	No
2	1.000	1.000	0.100	0.500	0.049	0.049	213415	No
32	1.250	1.250	0.100	0.625	0.102	0.102	128477	No
54	1.250	3.000	0.125	1.500	0.259	1.079	29182	No
68	1.500	2.000	0.100	1.000	0.233	0.368	57034	No
73	1.500	2.500	0.075	1.250	0.221	0.493	53233	No
81	1.500	3.000	0.125	1.500	0.396	1.209	26062	No
98	1.750	2.250	0.100	1.125	0.369	0.548	43084	No
119	2.000	1.750	0.100	0.875	0.413	0.335	54908	No
135	2.000	3.000	0.125	1.500	0.772	1.467	21471	No

The make up the carbon fiber tubes consist of an inner 45° Hex layup, a uniaxial fiber layer, and an out 45° hex layup as shown in Figure 8. Carbon fiber was chosen because of its high strength to weight ratio. Rectangular box sections were a good combination of strength along both axes and joint structures to be easily attached to the ends.

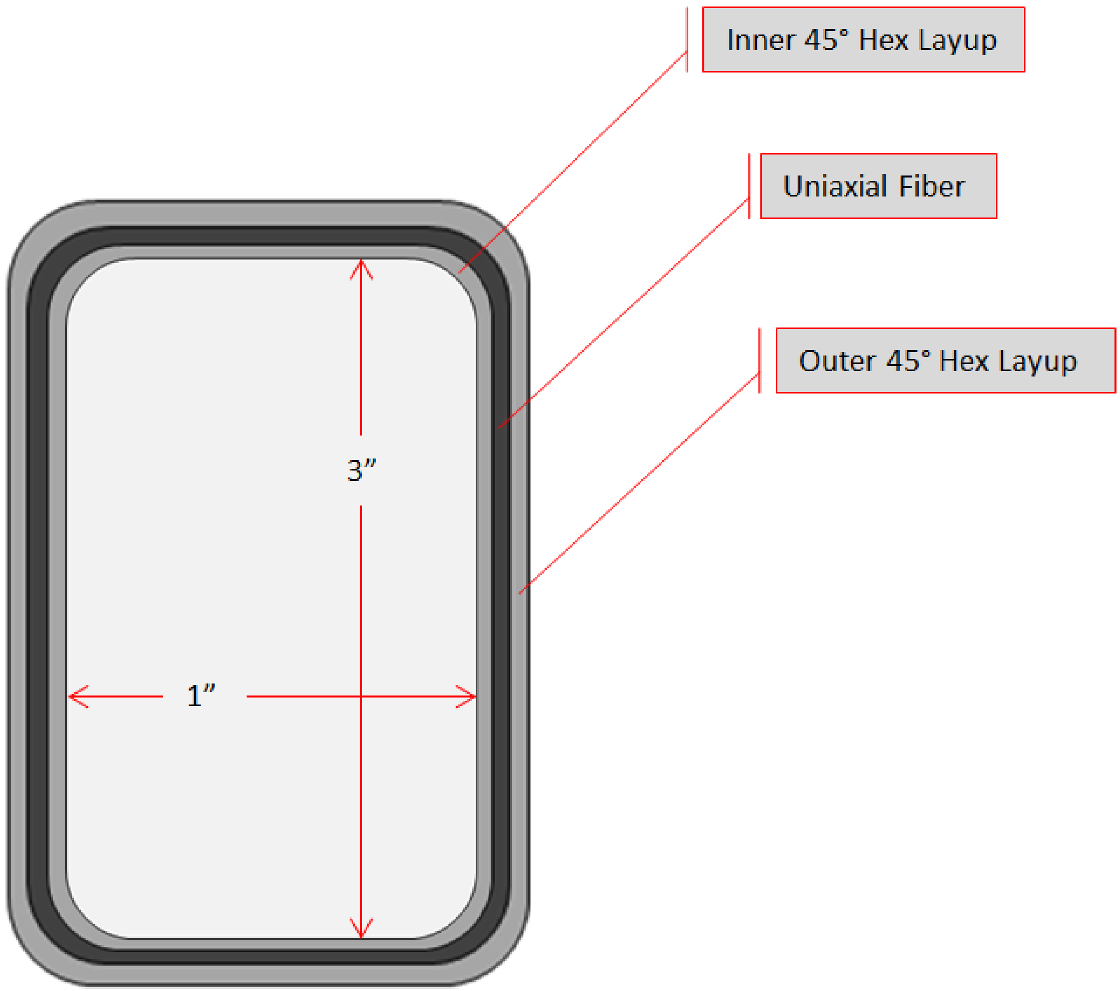

Figure 8: Make-Up of Carbon Fiber Tube. NOTE: Diagram is not to scale

Joints

The joints are aluminum end caps with a jigsaw puzzle piece resemblance that are attached to both ends of the carbon fiber box sections (see Figures 9 and 10). The joints slide together and are secured by T-handle locking pins as shown in Figure 11. The joints are designed to handle the bending loads of horizontal, vertical and angled deployment and are designed to directly load the carbon fiber box sections. The pins are strong in shear loading and prevent the rails from sliding once assembled. The T-handles allow a soldier to easily assemble the tool, quickly and accurately, while providing tactile feedback that the elements have been securely joined. To attach the joints to the carbon fiber tube, Loctite/Hysol 9430 Epoxy Structural adhesive was used. Loctite Hysol 9430 is formulated to give a combination of very high peel strength and is excellent in shear strength. The flexible nature of this adhesive makes it a perfect choice for bonding dissimilar materials including aluminum and carbon fiber [5].

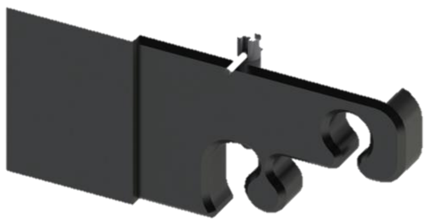

Figure 9: Pin and joint

Figure 10: T-handle locking pin

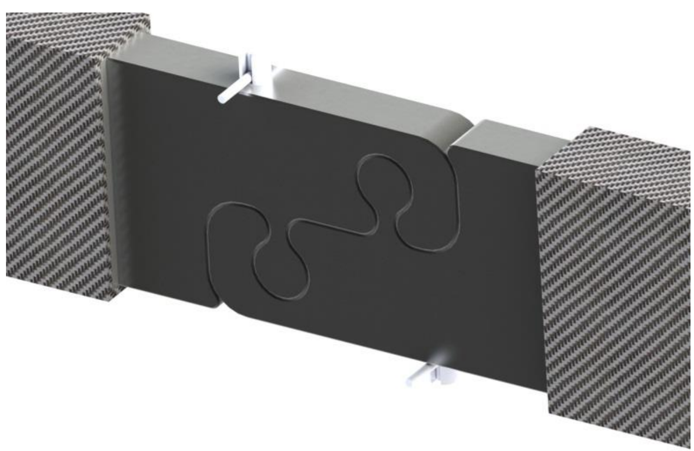

Figure 11: Joint connection

Slot

In each element, the carbon fiber tube has a 3" x 0.875" slot located in its middle. The slot in each element houses the element acting as the stepping rung. The aluminum joint of the rung element inserts into the slot of the rail element. Four guide posts are permanently built into the slots to serve multiple purposes. The initial intent was for the guide rails to aid in directing the aluminum end cap into the slot. The guide posts also have a secondary purpose of locking the rung in place when it is inserted into the slot. A detent was designed to be built into the guideposts in order to lock the rung in place. Due to time considerations the detents were not included in the bridge prototype.

When it comes to fabricating the slot, it is cut out of the carbon fiber using a 1/4'' carbite bit in a router. A 0.02-inch tolerance was used when designing the hole in order to assure that the aluminum end cap will always fit in the slot. The guideposts are inserted into the carbon fiber slot. The joint through the slot is shown below in Figure 12.

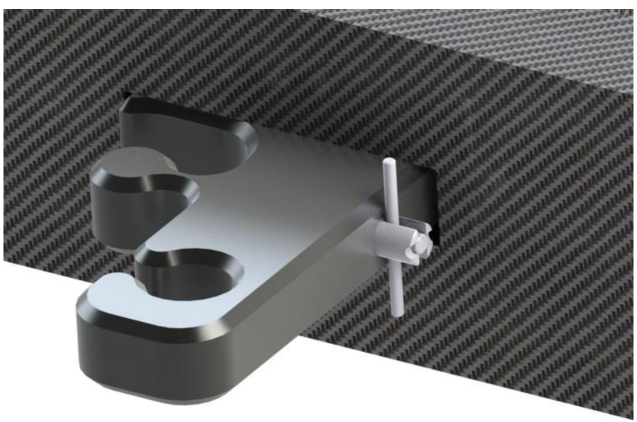

Figure 12: Slot assembly

Lighting

Due to time constraints and budgeting, the lighting system was not implemented on the prototype, although a scale model was constructed.

The lighting system is optimal in low-light situations, when night vision goggles are not being used and being spotted by an enemy is not of strong concern. The system may be easily switched off to avoid potential compromise of position. It is designed to work optimally based on the orientation of the device. The lighting requires minimal knowledge or action from the airmen in order to function. The lights are positioned above the rungs and oriented downward to aid in foot placement. The low-level lighting provides a confident feel for where the airmen need to step next.

Each uniform element of the bridge is designed to have its own self-contained electronic unit in order to maintain the symmetry of the overall device. There are three methods of sensing: a proximity sensor which detects when the rung is inserted into the slot, a small button on either side to determine which side is the inner side of the device where the light should shine, and a tilt switch which tells which side of the bridge is facing upward. The proximity sensor and side buttons only provide power while they are activated, so that the lights remain off until the pieces are connected. The tilt switch is activated within approximately ±45° degrees of the horizontal for each orientation. This allows a hands-free illumination of the lights when airmen are crossing the device and an automatic disengage when used as a ladder. This prevents the lights from activating when the structure is fully upright and appearing to the enemy as a beacon. A switch is implemented on each element to act as an overall kill switch. When the elements are connected, activating any kill switch will shut off power to all elements.

A small battery pack in each element powers the lights. This battery is channeled through a NAND gate directly through the kill switch and is connected to the rest of the elements (detailed below in Figure 13). The output from the NAND goes through the capacitive sensor, which sends power to the other switches when it is tripped. Each switch performs its desired function and the outputs are directed so that only one LED on each side piece is activated at a time, the top inner light. Figure 14 and Figure 15 below show detail of the wiring of the system and the placement of the LEDs, respectively.

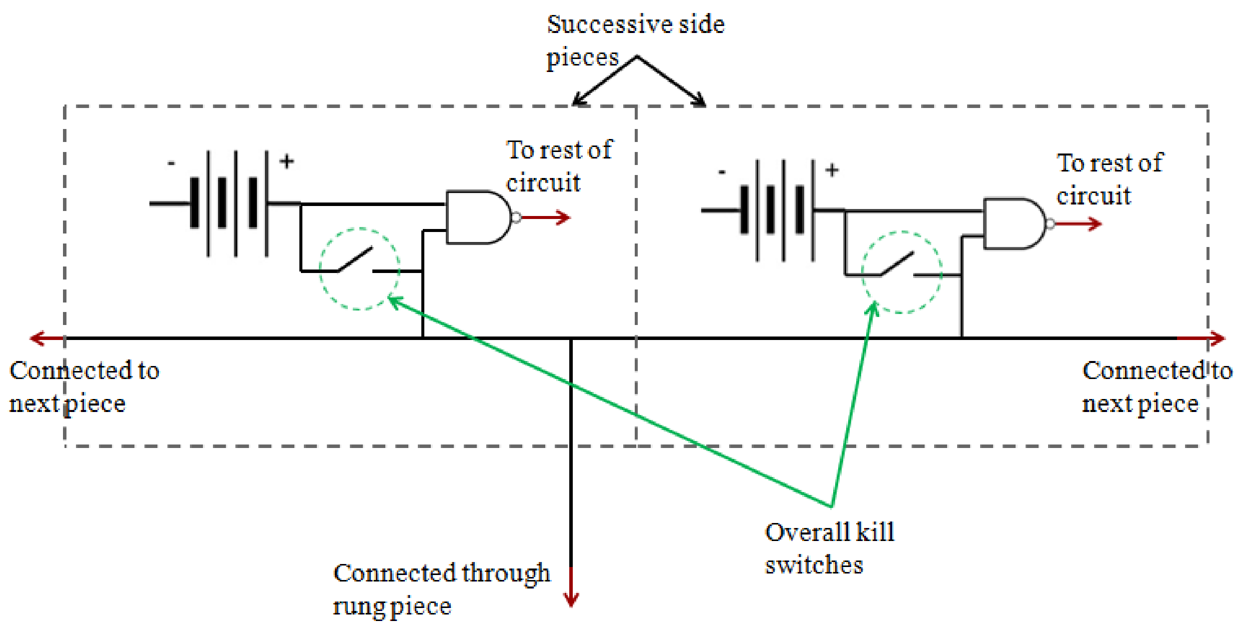

Figure 13: Conceptual Schematic of Kill Switches

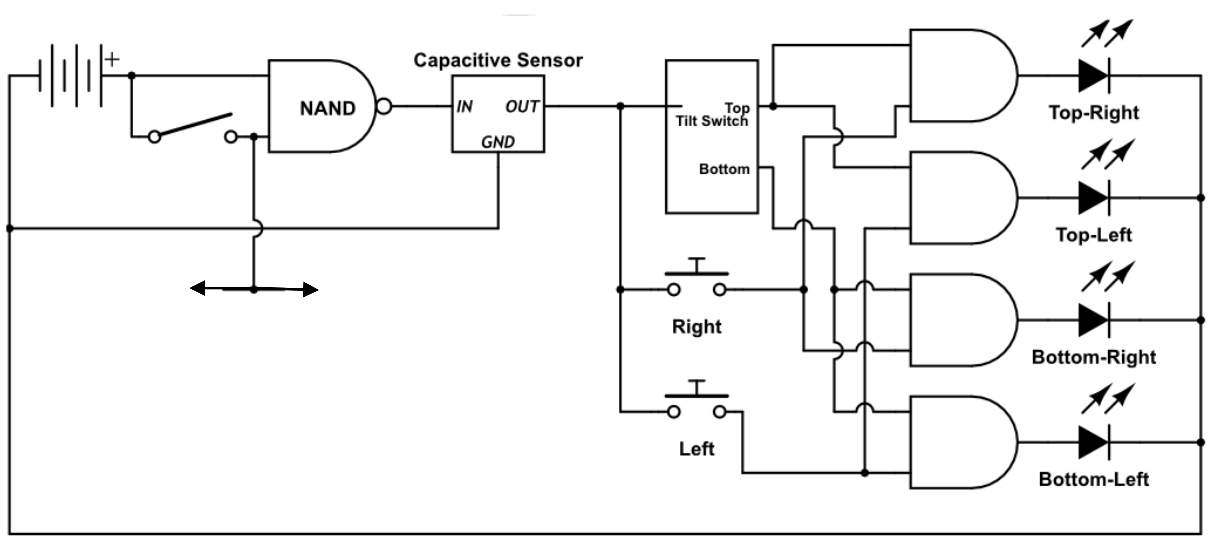

Figure 14: Basic Lighting Schematic

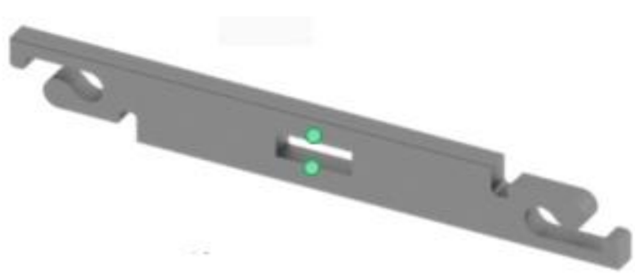

Figure 15: LED Positioning

The lights are low-intensity in order to minimize visibility from below or above from a distance. To avoid jeopardizing the airmen's position, green lights were chosen because it is a difficult color to detect with the use of night vision goggles (NVGs) that enemies might be wearing. A few other options were considered, but since the system needs to be low power, easily visible at close range, and not easily spotted at a distance or with NVGs, green was the preferred choice.

Figure 17: The airmen wear … operations. The lighting of the … with the use of the NVGs at a clos…

Figure 16: This helmet is an example of how the airmen wear the NVGs.

The design of the lighting contributes to the overall desire to remain unseen by the enemies. The color choice of the bridge is also essential in keeping the airmen unseen. The bridge has been painted Coyote Brown as it is the standard color used by the military in desert or jungle conditions.

Stabilizer

An end stabilizer was built to add stability to the bridge and prevent tipping in the case of eccentric loads on the bridge. The main structure of the stabilizer is constructed out of a 1" x 2" aluminum box section, cut into two 2-foot lengths. These two pieces are assembled and secured using a pin to create a 4-foot piece that acts as a base for the bridge.

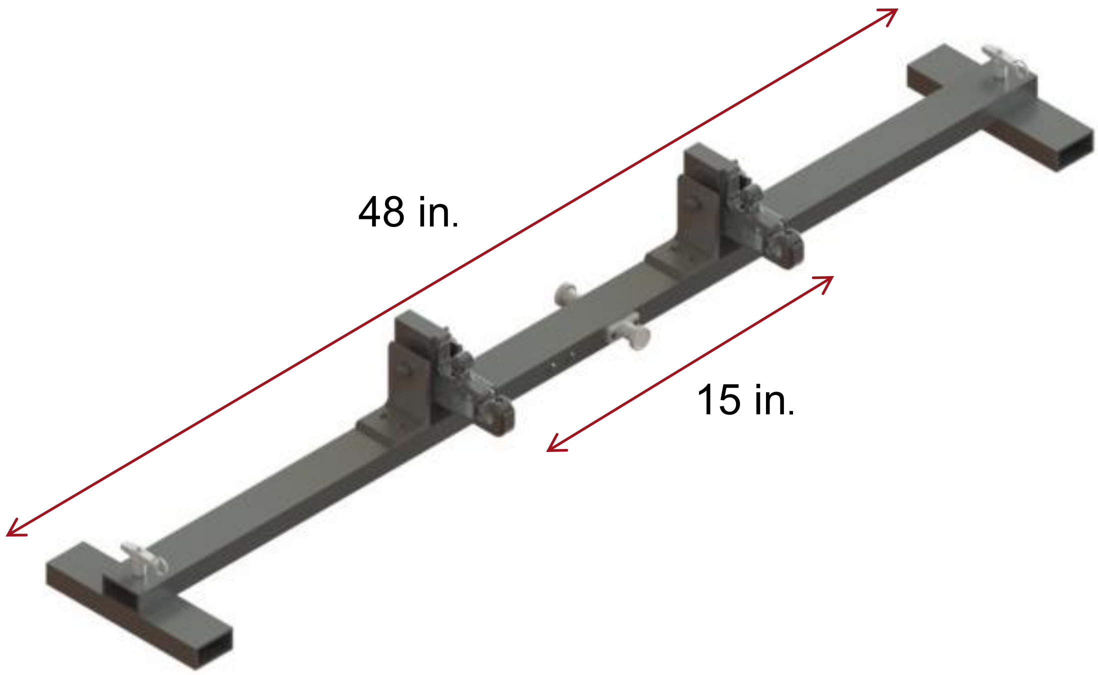

Figure 18: Main Structure of Stabilizer

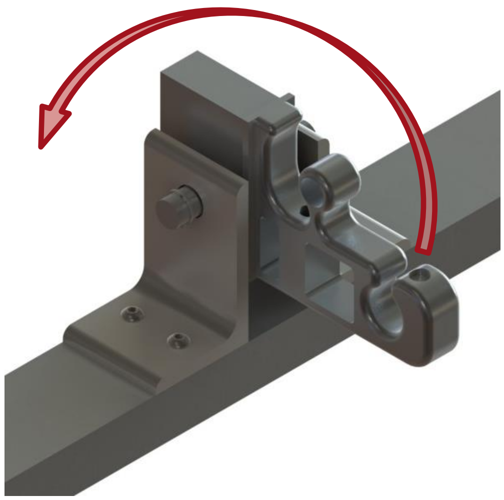

Figure 19: Rotating Joint

The bridge is attached to the stabilizer via a bridge joint which is permanently mounted onto the stabilizer. Two L-brackets with a shaft going through them secure this joint to the bridge and allow it to rotate, enabling both horizontal and vertical use. Retaining rings are used to keep the shaft from sliding out. With more time for design and manufacturing, small turntables or bearings would be used to mount the L-brackets so that they could rotate and allow for either joint orientation (pointing up or pointing down). This would maintain the overall flexibility in the assembly process, allowing for the bridge to be attached to the stabilizer regardless of how the bridge was assembled.

Eight-inch pieces of the 1” x 2” box section were used to create feet for the stabilizer. One of these pieces would attach to both ends of the stabilizer. Three different versions of the feet were designed to account for different surfaces that may be encountered in the field. For sand and ice, feet with sharp metal spikes on the bottom would be used. For dirt or mud, feet with baseball style (flat bottom) spikes would be used. For rock or concrete, feet with textured rubber pads adhesively attached to the bottom would be used. On the feet that use spikes, threaded holes would be drilled out of the bottoms of the feet so that the spikes could simply be screwed in.

The “foot” pieces would each have two bolts coming out of the top of them that would be glued into place, with the heads of the bolts sticking out. To attach the “feet” to the stabilizer, the heads of these bolts would be inserted into slotted holes on the bottom of the stabilizer. The “feet” would then slide over so that the bolts moved into the thinner portion of the slotted hole and the heads would no longer be able to pass out of the hole. A pin would then be dropped through the main box section and the top of the “foot” piece to keep the “foot” from sliding back toward the larger portion of the slotted hole and detaching.

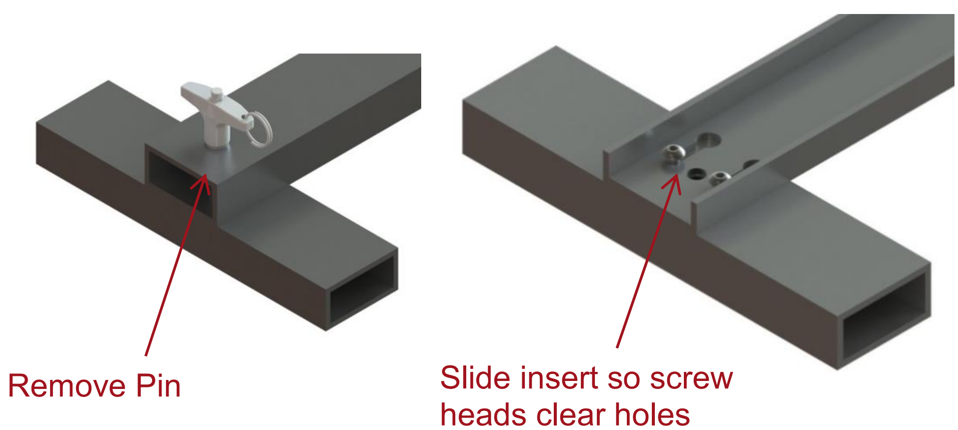

Figure 20: Interchangeable insert held by pin and cap screws for quick changing

Figure 21: Plastic Cleats

Figure 22: Rubber Pads

Figure 23: Metal Spikes

The Bridge: Assembly & Use

When the airmen encounter an obstacle, a rough estimate of the crossing distance is made. The device is assembled into H-shaped increments, which requires three elements. An initial "H" is made by sliding an aluminum joint through the slot of another element, creating a "T" shape. To secure the joints through the slot, carabineers are attached through the small rectangular hole of the joint, shown in FIGURE below. Then the other aluminum joint is slid through the slot of the third element, forming an H-shape. To ensure the bridge is compatible with the stabilizer, the third element orientation must mimic the orientation of the first element. From this point on, each element is added to the previous "H" shape in the 1, 2, 3 order displayed below in Figure 24.

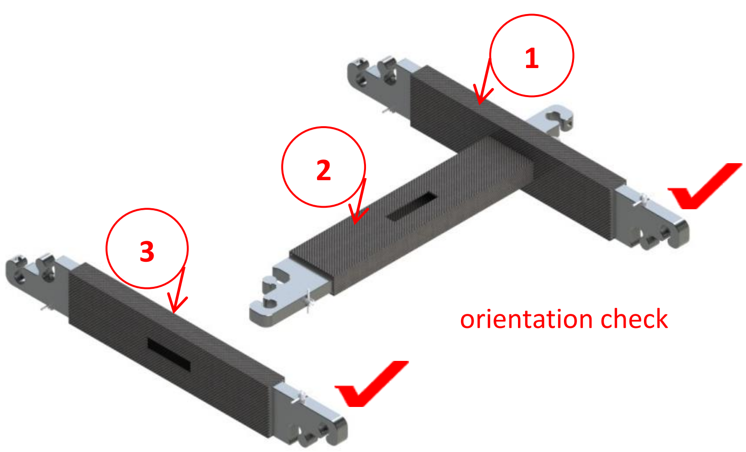

Figure 24: 1, 2, 3 "H" Assembly Method

See **Error! Reference source not found.** through **Error! Reference source not found.** below for step-by-step assembly instructions of the bridge elements.

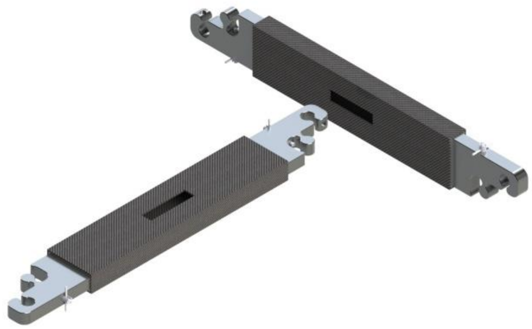

Figure 25: Assembly: STEP 1

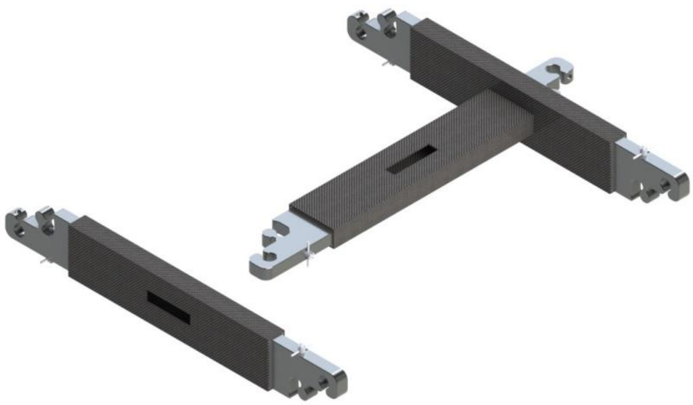

Figure 26: Assembly STEP 2

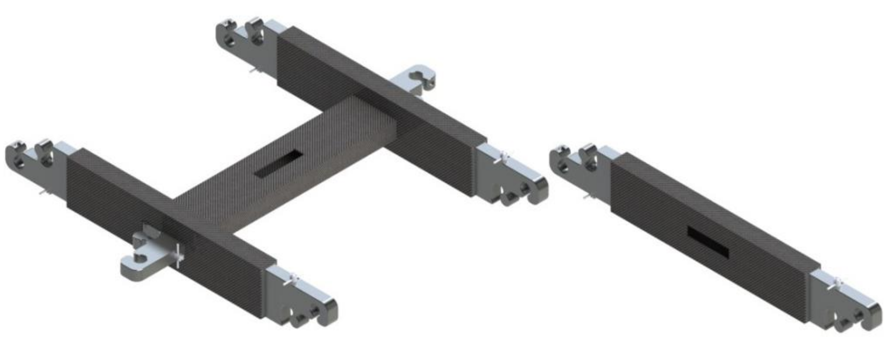

Figure 27: Assembly: STEP 3

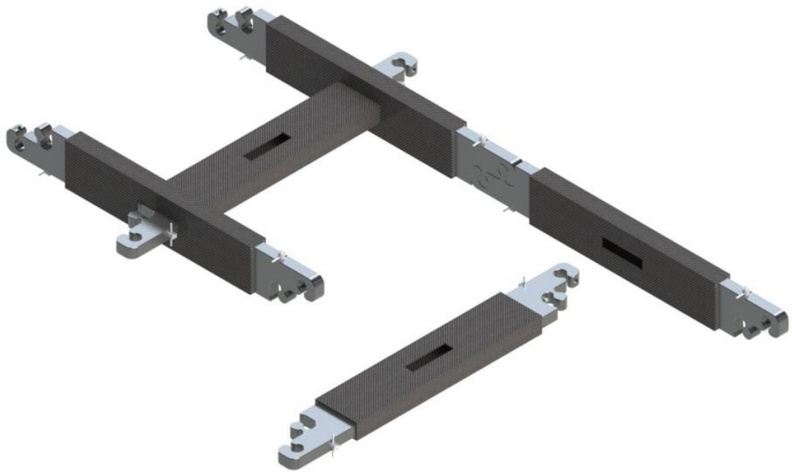

Figure 28: Assembly: STEP 4

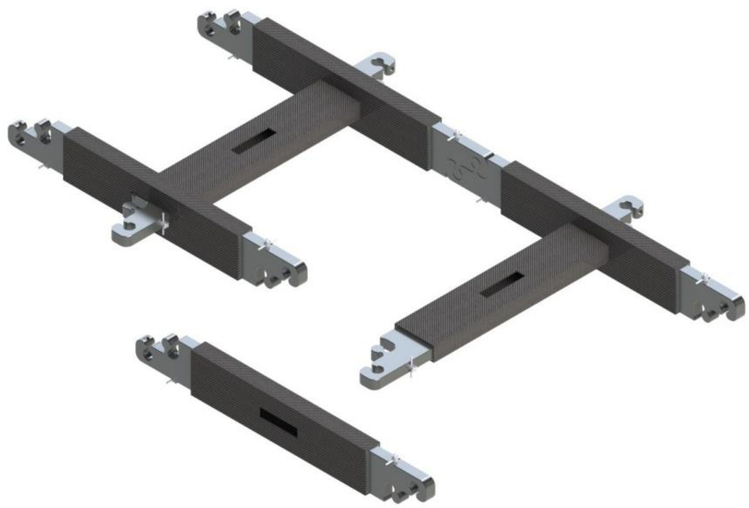

Figure 29: Assembly: STEP 5

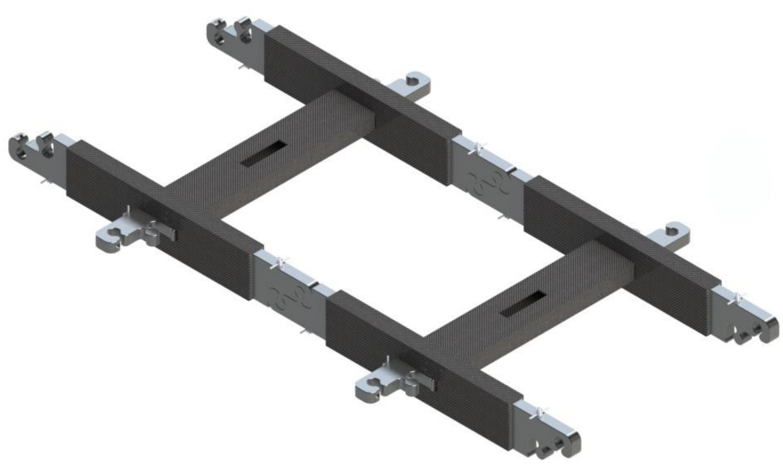

Figure 30: Assembly: STEP 6

The detailed description of the assembly of two joints has been explained previously in the “Joints” chapter. Once the joints are connected, engage the safety lock by turning the T-handle lock a quarter turn in any direction.

Once the bridge has been assembled to the desired crossing distance, the stabilizer can be attached as mentioned in the “Stabilizer” chapter above. Due to the large length and weight of the bridge, dropping the bridge over an obstacle is possible, but not always ideal. Various methods in deploying the bridge depend on the obstacle being faced.

A common obstacle airmen come across during an operation roof top to roof top. To safely deploy the bridge across an obstacle like that, a drawbridge type deployment is suggested. To deploy the bridge, a rope is tied to the free end. Positioning the bridge vertically, an airman props their foot on the stabilizer of the grounded end while gripping the untied end of the rope. The airman gradually releases rope to lower the bridge. Once the bridge is deployed horizontally, the airman ties the free end of the rope to the grounded stabilizer. After this has been completed, the airmen traverse across the bridge. To bring the bridge to the new side, the tied rope from the free end is untied. An airman props their foot on the stabilizer of the free end and slowly pulls the rope towards their self, bringing the bridge to a vertical position to then be disassembled.

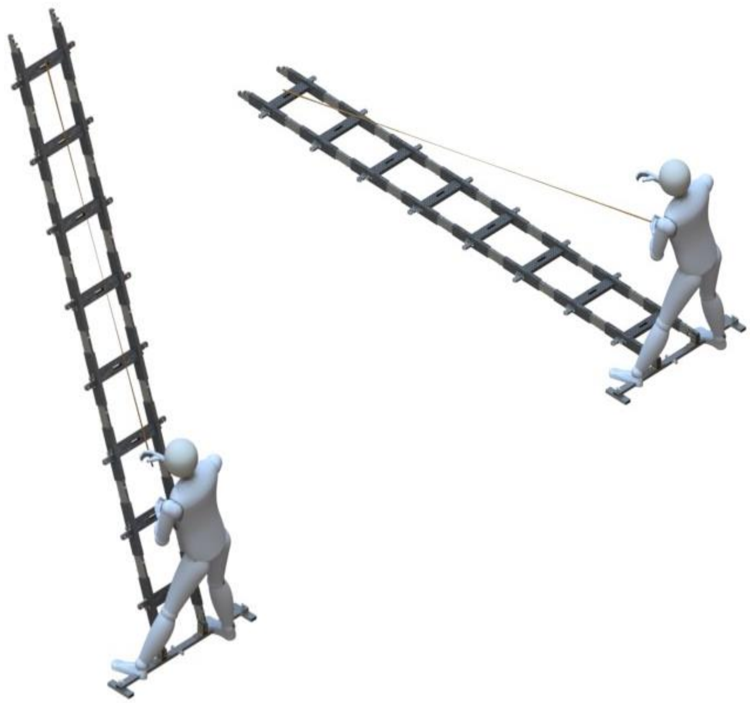

Figure 31: Deployment Demonstration

Various assembly processes exist that coincide with specific obstacles. For example, crossing between two buildings on the third floor from one window to the other does not allow for a drawbridge deployment. Now consider the crossing distance is larger than the size of the room the airmen are in, here lies an additional constraint when having to deploy the bridge. To face this obstacle, the airmen would assemble the bridge as described above ("H" method). With each additional "H" added to the bridge, airmen would shuffle the bridge out the window and complete the assembly process when the bridge reaches the other window.

For a vertical obstacle, say from the ground to the third floor window, only one stabilizer is needed at the base of the device. A similar assembly and deployment process is implemented as described for the drawbridge deployment of horizontal obstacles.

In many instances airmen face obstacles that are vertical and horizontal, such as a shorter rooftop to a tall rooftop. In this case, two stabilizers would be used to brace each end on either surface. The assembly would be the “H” method and the deployment would be the drawbridge method.

The device takes approximately ___ minutes for a single Battlefield Airmen to assemble and __ minutes(deleted). If two airmen were available to set up the device, the assembly time would decrease to ___ minutes. The assembly time is inversely proportional to the amount of airmen available to assist in deployment until optimal conditions are met. The optimal number of airmen assembling the device is ___. When there are four airmen assembling the bridge, it is ideal to start with the H-shape and have two teams of two airmen assemble from either end of the initial H-shape. (deleted) Testing was performed to validate the assembly time of the device under various conditions. The time frames mentioned above are under the assumption of perfect conditions. Wet conditions and night conditions were also tested. Result averages are tabulated in Table 4 below.

Table 4: Average Assembly Time under Various Conditions

Condition	Time (s)
Perfect	
Wet	
Night	

To disassemble the bridge, the carabineers are taken off first. The rails are then removed from either side of the rungs. Once the rails are removed, each element is unfastened by disengaging the T-handles. All the elements are free from each other and may be packed into the rucksack. The disassembly time using this method with four people is ____. FIGURE through FIGURE show the disassembly method.

As depicted in Figure 32 the ideal packing volume of one cubic foot in its compacted form. The packaged front view is shown in Figure 33 below.

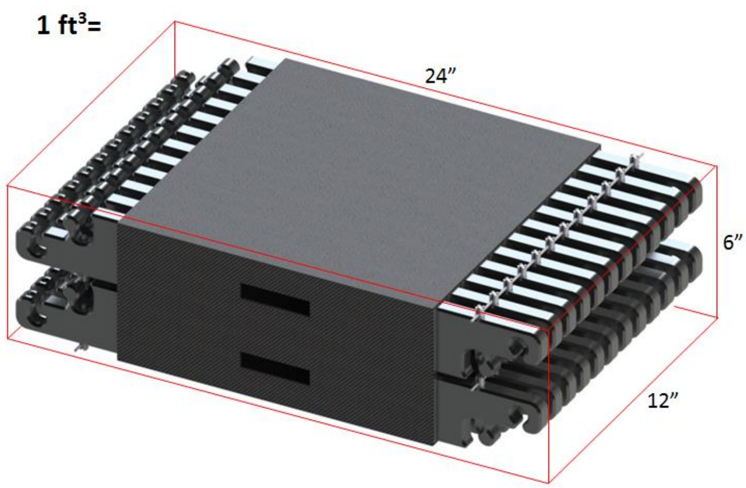

Figure 32: Isometric view of packaged volume (NOTE: not to scale)

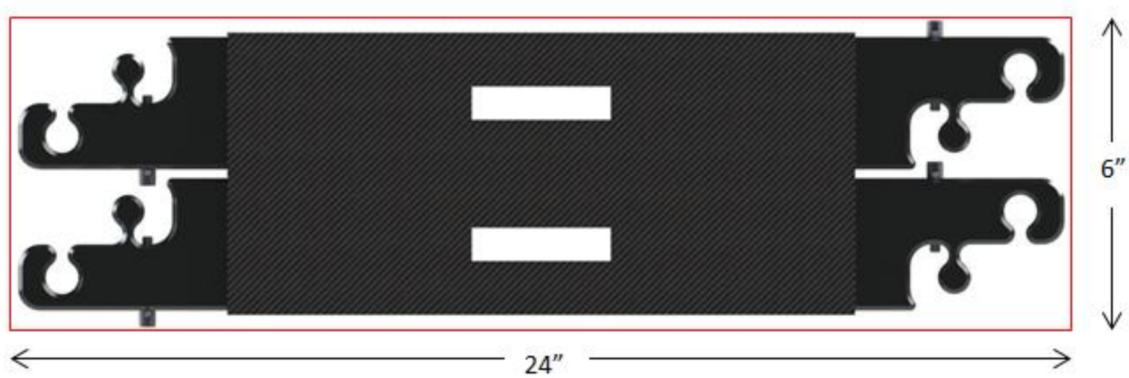

Figure 33: Front view of packaged volume (NOTE: not to scale)

A package test was performed to measure the packing volume of the device in comparison to the ideal scenario. The compacted device was placed into a 12” x 24” x 6” prefabricated rectangular prism and measurements were taken and recorded for the length, width and height. See Table 5 below for the results. The T-handle pins add ___ inch to the ideal 6” measurement.

Table 5: Dimensions of Compacted Bridge

Length	Width	Height
	IN PROGRESS	

The Bridge: Detailed Analysis

Weight

Due to time constraints and manufacturing limitations, many of the weight saving features in the joints are not incorporated into the working prototype. Consequently, the actual overall prototype weight will be considerably higher than the ideal device weight. The ideal weight of the device is 52.6 pounds; this number does not include the stabilizer. The stabilizer itself weighs _____ pounds. A simple test was performed to measure the actual weight of the device by placing it on a calibrated scale and recording the value once the scale reached equilibrium. Multiple iterations were performed to decrease procedure and human error. Results showed that the actual weight of the prototype is 54 lbs.

Strength: Sizing of Bridge Components

When performing the structural analysis, the two most dominant modes of failure are yielding due to the overall bending stress and vertical buckling. It was crucial that the goal of supporting a 350 pound load was met and ideally exceeded for each module. Other failure modes considered are the following: deformation, bending in joint, bending in the rung of a single bridge segment, bending of the rail in a single bridge segment, local horizontal buckling of the total bridge, stress concentration, pin shear and adhesive shear. For justification of any calculated numbers that follow, reference Appendix D: Sample Calculations.

Material Properties

The Ohio State Bridge is composed of two main materials: carbon fiber and aluminum. The material properties of each are listed on Tables 6 and 7 below. These values are used in many of the structural analysis calculations.

Table 6: Standard Properties of Carbon Fiber

Yield Stress	310 ksi

Table 7: Standard Properties of Aluminum 6061

Modulus of Elasticity	10.3 x 10^6 psi
Yield Stress	14.9 ksi

Overall Bending Stress

A majority of the strength calculations are based on the assumption that the bridge, as a whole, is modeled as a simply supported beam with a concentrated load at its center. This case is depicted in Figure 30 below. Under such assumptions, the reaction forces, load, maximum shear and maximum moment are determined using Equations 1, 2, and 3 below.

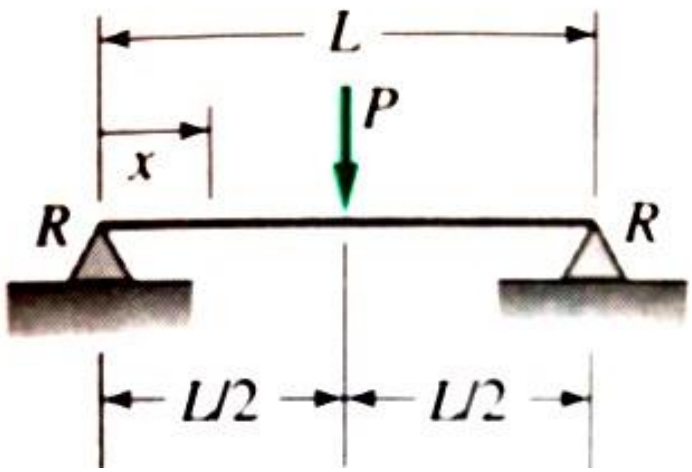

Figure 34: Simply Supported Beam with Load Concentrated at Center [1]

$$R = \frac{P}{2} \quad (1)$$

$$V_{max} = \pm \frac{P}{2} \quad (2)$$

$$M_{max} = \frac{PL}{4} \quad (3)$$

R = Reaction force

P = Load seen by a single rail
V_{max} = Maximum shear force
L = Length of beam
M_{max}= Maximum moment

The reaction force is half of the total load seen by a single rail or 87.5 pounds. Such a reaction force yields a maximum shear of 87.5 pounds and a maximum moment of 10,500 pound-inches.

The box section of the carbon fiber is subject to bending, which is a potential failure mode. Analysis was completed in order to ensure the bending stress seen by the box section is less than that of its yield strength. Equation 4 was used to calculate the overall bending stress. The structure was analyzed at a maximum crossing length of 20 feet, and was modeled as a simply supported beam that is loaded with 175 pounds at its center.

$$\sigma = \frac{Mc}{I} \tag{4}$$

M = Maximum bending moment
c = Perpendicular distance to the neutral axis
I = Moment of inertia

From Equation 4, the maximum bending stress on the bridge is 25.7 ksi. Many different cross-sections met the aforementioned loading conditions without failing. To further narrow down the possible cross-sections, consideration was given to packing volume and material weight. After deliberation, the optimum dimensions were determined to be a 3” x 1” cross section with a 0.1 to 0.125 inch wall thickness. Due to time constraints and lack of material availability, the actual prototype has a 1.25” x 3.25” cross section with a 0.125 inch wall thickness. For detailed calculation, reference spreadsheet in Appendix D.

Deformation

Deformation analysis was performed in order to instill a sense of stability in the soldiers crossing the bridge. For calculation purposes, the bridge was modeled as a uniform beam with a load of 350 lbs concentrated at its center. The associated beam deflection is given in Equation 5 below.

$$\delta_{max} = \frac{PL^3}{48EI_x} \quad (5)$$

δ_{max} = Deflection of bridge

L = Length of bridge

P = Load

E = Modulus of Elasticity for Aluminum

I_x = Moment of Inertia about the bending axis

The resulting maximum deflection for a 10 foot bridge is 0.198 inches. The resulting maximum deflection for a 20 foot bridge is 1.58 inches. This span is achieved by connecting two 10 foot bridges. The majority of deflection occurs in the tolerance gaps of the puzzle piece joints as opposed to the carbon fiber.

Necking

Each puzzle piece joint connection is subjected to a couple-moment, previously determined to be 10,500 lb-in. When looking at the free body diagram of a single joint the 10,500 lb-in moment is translated to a force-couple about the axis, as displayed in Figure 32. The magnitude of the couple force was calculated to be 7000 lb by dividing the moment by the length of the moment arm.

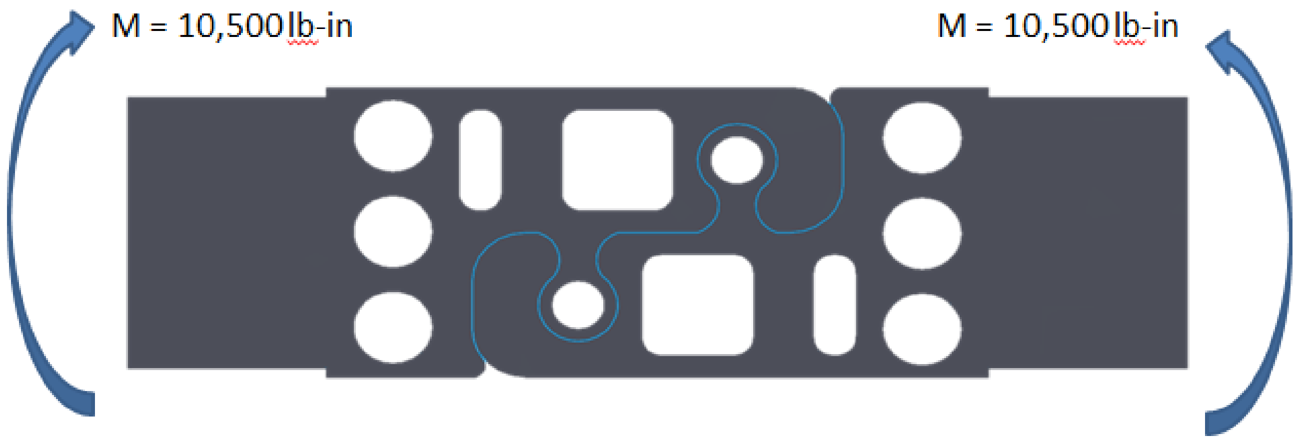

Figure 35: Free Body Diagram of Joint Connection

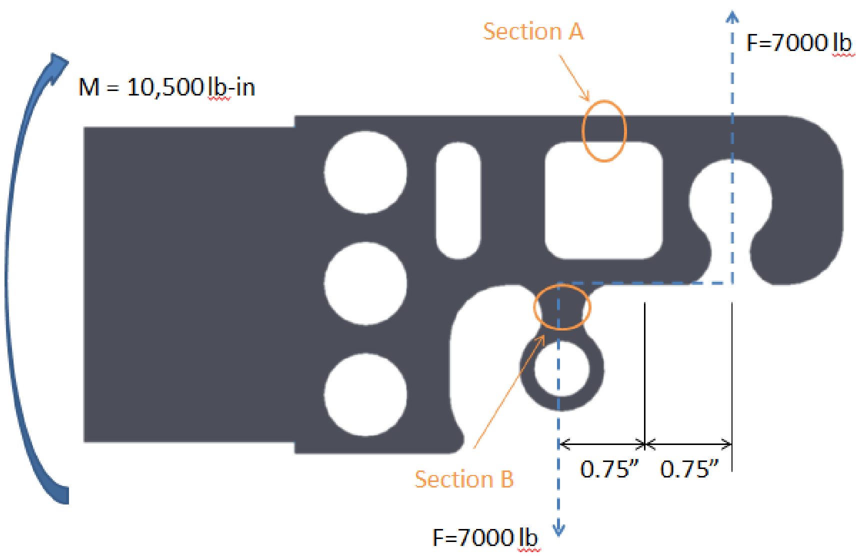

Figure 36: Free Body Diagram of Single Joint in Bending

There are two critical areas of the joint geometry that are subject to failure; these are labeled as Section A and Section B in Figure 32 above. Section A is analyzed using FEA due to unknown loading conditions and complex geometries. Section B is subject to necking. The stress due to necking was calculated to be 31.1 ksi using Equation 6. The ultimate tensile strength of aluminum is 71 ksi, yielding a factor of safety of 2.3.

$$\sigma_{neck} = \frac{F}{A} \tag{6}$$

Bending Stress in a Single Bridge Segment

A variation of the bending equation used in the previous two bending analysis was also used to determine the bending stress in the rails and rungs of a single component. Refer to Equations 7 and 8 below.

$$\sigma_{Rail} = \frac{M_{max} c_y}{I_x} \qquad (7)$$

σ_{Rail}= bending stress in the rail

M_{max} = Maximum bending moment of the rail

c_y = perpendicular distance to the neutral axis

I_x = moment of inertia of the rail

$$\sigma_{Rung} = \frac{M_{max} c_x}{I_y} \qquad (8)$$

σ_{Rung}= bending stress in the rung

M_{max} = Maximum bending moment of the rung

c_x = perpendicular distance to the neutral axis

I_y = moment of inertia of the rung

The bending stress in the rail of a single component is 12.9 ksi and the bending stress in the rung of a single component is 23.5 ksi. Both values are significantly lower than the bending strength of carbon fiber; therefore, the bridge will not fail under bending of a single bridge segment.

Buckling – Locally

For local buckling failure, the critical load is given by Equation 9. A few parameters must first be determined before a critical load can be calculated. Instead of looking at the cross section as a whole, the walls are modeled as fixed-fixed beams. For the case where the beam is fixed at both ends, the effective length is half of the total length. Under such conditions, the buckling constant K_h is 16.93 [1]. The Shear Modulus of aluminum is 3900 ksi.

$$F_{crit} = \frac{K_h}{{L_e}^2}\sqrt{EI_yGJ_e} \qquad 9$$

$\boldsymbol{F_{crit}}$ = Horizontal critical buckling load

K_h = Buckling Constant under horizontal loading conditions

L_e = Effective length or height of rail

E = Young's Modulus of Elasticity of carbon fiber

I_y = Moment of Inertia about the vertical axis

G = Shear Modulus

J_e = Property of cross section relating to torque and angle of twist

The horizontal local buckling of the rail will occur at a resulting critical load of 26.5 kip; whereas the horizontal local buckling of the rung will occur at a critical load of 1646 kip. Between the two, the rail will be the first to buckle locally when the bridge is oriented purely horizontal. However, these values are considerably high than the allowable loads dictated by the other failure modes. Therefore, local buckling as a potential failure may be ignored.

Buckling – Vertical

Vertical buckling failure is a concern due to the significantly large span length of 20 ft. When the device is deployed in the vertical direction, the side rails act as fixed-free beams. For this case, the effective length of the bridge is twice the total bridge length or 480 inches. The critical load is determined using Equation 10 below.

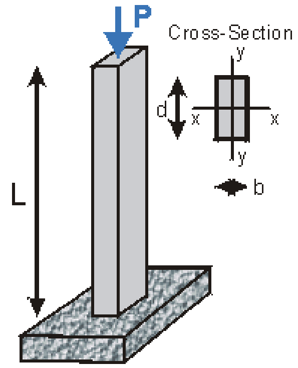

Figure 37: Vertical Buckling

$$F_{crit} = \frac{K_v}{{L_e}^2}\sqrt{EI_xGJ_e} \qquad 10$$

$\boldsymbol{F_{crit}}$ = Vertical critical buckling load

K_v = Buckling Constant under vertical loading conditions

L_e = Effective length of total bridge

E = Young's Modulus of Elasticity of carbon fiber

I_y = Moment of Inertia about the horizontal axis

G = Shear Modulus

J_e = Property of cross section relating to torque and angle of twist

The critical load is maximized for the case where the angle between the device and datum is oriented 90 degrees. Although, this is not practical in application it is used as a worst case scenario. Under this assumption, the critical buckling load is 3.16 kip.

Shear in Pin

A calculation was performed to evaluate shearing in a single pin. As shown in Equation 11, shear stress is found by dividing a load by a cross-sectional area. For shear, the cross sectional area is an inner profile of a cylinder with diameter 0.233 and height 0.375. A load of 350 pounds is assumed to be concentrated at the center of the pin.

###Pending Figure of Cross Section###

$$V_{pin} = \frac{P}{A_{pin}} \qquad 11$$

V_{pin} = Shear in the pin

P = Load

A_{pin} = Cross sectional area of pin

The shear stress in the pin is 2.55 ksi. Comparing the shear stress to the shear strength of the pin concludes that the pin will not fail due to shear.

Adhesive Bonding

For preliminary design purposes, the average shearing stress in the adhesive layer is calculated and multiplied by a stress distribution factor, as displayed in Equation 12 below. As Figure 35 shows, a single adhesively bonded lap joint is considered. The epoxy only sees a load in the axial direction. In the absence of specific data, a stress distribution factor of 2 is utilized as it is the worst case scenario [1].

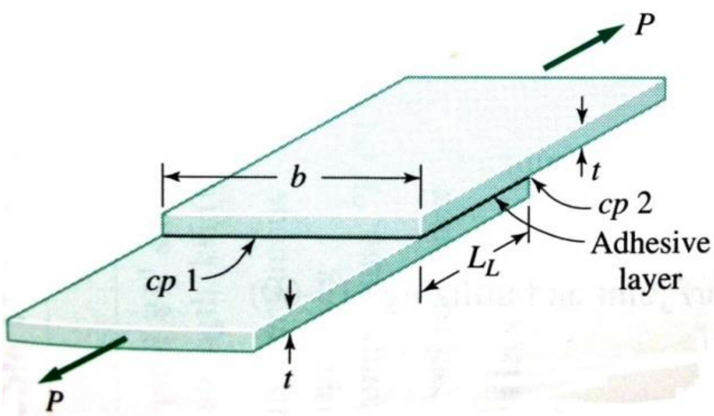

Figure 38: Adhesively bonded lap joint [1]

$$\tau_{max} = \kappa_s \tau_{ave} = \kappa_s \left(\frac{P}{bL_L}\right) \quad 12$$

κ_s=stress distribution factor

P= applied load in the axial direction

b= width of adhesive layer

L_L= length of adhesive layer

Plugging in values into Equation 12 yields a maximum shearing stress of nearly 97 psi. Hysol 9430 Epoxy Adhesive's maximum allowable shear strength is 4700 psi. Since the maximum shearing stress observed is an order of magnitude less than the allowable, shear in adhesive bonding is ruled out as a potential failure mode.

Usability & Ergonomics

Considering the usability and ergonomics of the tool was a necessity. The airmen will not use equipment in combat that puts their safety at risk. If the tool is confusing to use or assemble, the airmen will not bother spending an extended amount of time figuring it out, especially if it compromises their safety. Therefore, the goal was to "keep it simple, stupid" and produce a tool designed for the airmen and their specific needs.

To ensure the ergonomics of the device would meet the airmen's needs, a professional opinion was necessary. Dr. Carolyn Sommerich, a professor at The Ohio State University and a professional in ergonomics, proved to be an excellent source. Dr. Sommerich stressed that symmetry is preferred when designing the components of the device. Full symmetry allows the airmen to grab any part in the rucksack and continue the assembly without any hesitation or confusion. Dr. Sommerich also emphasized the design must be simple. It is of the utmost importance that designs achieve the desired task in the easiest, simplest way possible. According to her, many tools that are put on the market today are often over-designed, which deter from the original goal and use of the product.

Simplicity and uniformity were in the frontline when deciding on a final design. It was decided to design the device that was completely symmetrical and had identical parts. The side rails and the rungs are the same element.

It was important to test the theory that symmetrical and identical parts contribute to a flawless and quick assembly. One of the most helpful methods to test this was in our beta testing. This test consisted of asking a number of people who had never came in contact with the device before to assemble the bridge with little or no direction. After observing their behaviors and obtaining their feedback, it was concluded that symmetry and uniformity played an essential role in a quick assembly time.

The Bridge: Interoperability

The bridge is designed to be multipurpose when the airmen are on missions. A table function is possible with the addition of one unique joint piece, shown is Figure 39 below. The assembled table is shown in Figure 40. Having the bridge be used as a table allows for a raised working surface or holding injured personnel.

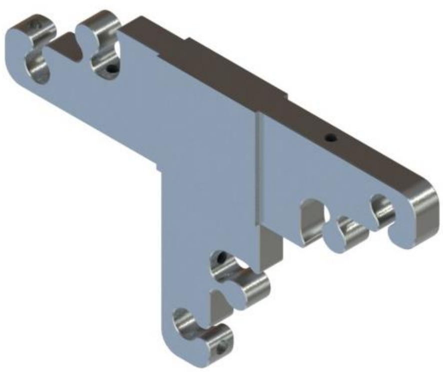

Figure 39: Three-Way Joint

Figure 40: Table Feature with 2 Three-Way Joints

The bridge could also be used for rappelling from an upper floor window. The airmen would assemble enough of the bridge to place against the inside of the window frame.

The drawbridge rope could then be tied to a rung. The airmen would then rappel down. Figure 41 below displays this feature of the bridge.

Figure 41: SHOW WITH WINDOW

The basic shape of the bridge allows it to be used as a stretcheer to carry injured personnel. The number of elements assembled is dependent of the size of the injured person. Figure 42 below demonstrates this feature.

Figure 42: Stretcher Feature

Conclusion

The Ohio State Bridge serves as the device Battlefield Airmen need to traverse the numerous obstacles encountered during special operations. The packaged volume is ___, which meets the design goal given by Master Sergeant Bean. This volume represents the contents of one rucksack. Using one rucksack, the airmen are able to cross obstacles up to 12.5 feet. With two rucksacks, the crossing span doubles, allowing the airmen to traverse obstacles up to 25 feet. The weight of the bridge is ___. The 12.5 ft bridge is able to withstand ___ static load and ___ dynamic load with a safety factor of ____. With an assembly time of ___**,** lighting feature, and stabilizer, the Ohio State Bridge is a substantially strong and safe device that Battlefield Airmen will trust during their operations. With any prototype, there is room for improvement before a final product is ready for mass production. The weight of the bridge would be reduced by using lighter material researched by the government, adding weight-saving features into the joint, and reducing the overall size of the bridge. Furthermore, the stabilizer would be modified to be compact, orientation adaptable, and provide various surface accessories to adapt to all terrain faced by the airmen. The final product would also include joints that had locking fasteners built into them so the rungs attach and lock into the slots. Additionally, rivets would be used as back up to the Epoxy adhesive between the carbon fiber tubes and aluminum joints. In conclusion, the Ohio State University team appreciated the opportunity given by the Air Force Research Lab to design a bridge that could be used during special operations.

Appendix A – References

1. Force, U.S.A. *Battlefield Airmen*. 2013; Available from: http://m.airforce.com/joining-the-air-force/technical-training/battlefield-airmen.
2. Laboratory, A.F.R. *AFRL Challenge*. The Challenge 2013; Available from: http://afrlchallenge.org/theStakes.aspx?challengeID=9.
3. Force, N.M.o.t.U.A. *Pararescuemen and Combat Rescue Officers*. 1/9/2009 3/29/2013]; Available from: http://www.nationalmuseum.af.mil/factsheets/factsheet.asp?id=13581]. .
4. Force, N.M.o.t.U.A. *Special Operations Weather Technicians and Officers*. 1/19/2012; Available from: http://www.nationalmuseum.af.mil/factsheets/factsheet.asp?id=13581]. .
5. **Chemical-Supermarket.com**. *Loctite/Hysol 9430 Epoxy Structural Adhesive #203-403*. April 2, 2013]; Available from: http://www.chemical-supermarket.com/Loctite_Hysol_9430_Epoxy_Structural_Adhesive-p96.html.

Appendix B – Conceptual Designs

Connect Four

Ease of deployment, quick assembly, and uniform sections were the focus of this design. The design consisted of two variations: rotating rungs and pin-in-slot rungs. Overall, it did not meet the design focus of size and weight, as well as simplicity.

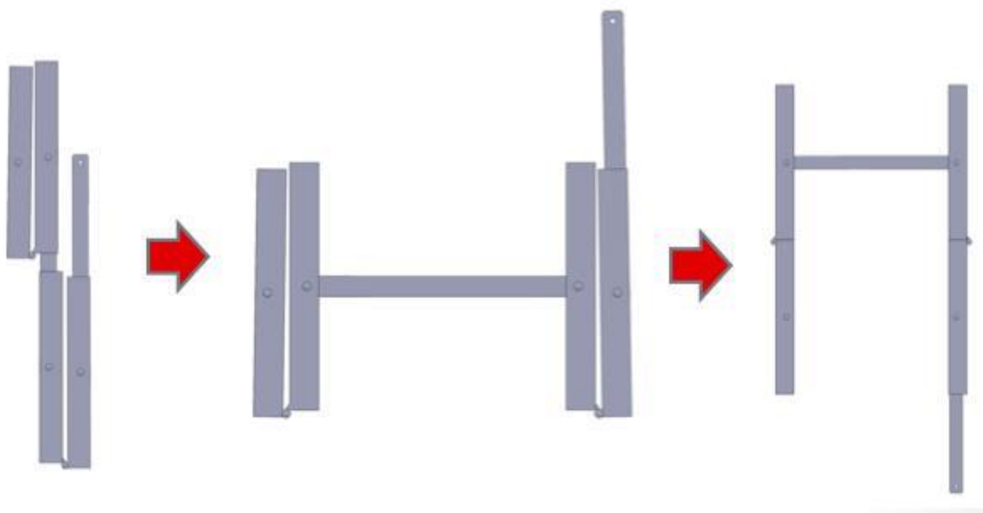

Figure 43: Connect Four Design

JL Mach

This design was collapsible and had a uniform assembly. The design fit in the 1 cubic foot volume requirement. The weight was estimated at 50 pounds with 80% of the design material being carbon fiber and had a crossing distance of ten feet. The figure below shows the part list that made up the design. The team's decision to discontinue with this design was due to the multiple parts, lack of simplicity, and the weight of the tool.

Figure 44: Components of JL Mach

Figure 45: JL Mach Design

Tapered Interconnect Bridge

The main structure was constructed of carbon fiber tubes while interconnects are tapered aluminum pins. Each rail had a male and female end. Top/bottom and left/right was important. The possibility of assembling it incorrectly was a high risk. This factor is why this design was discontinued.

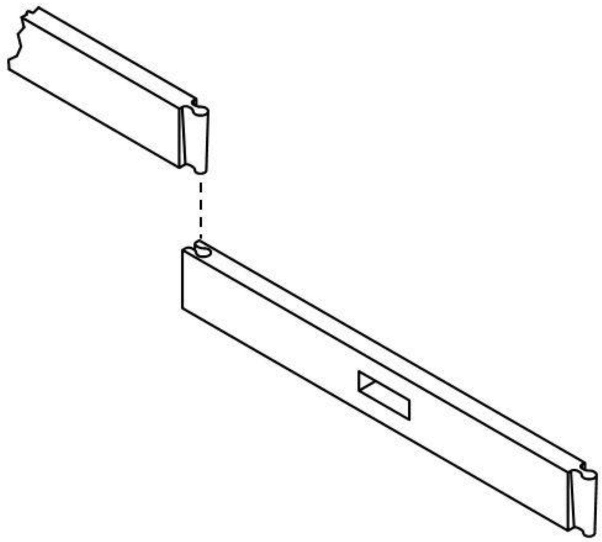

Figure 46: Tapered Interconnect Bridge Design

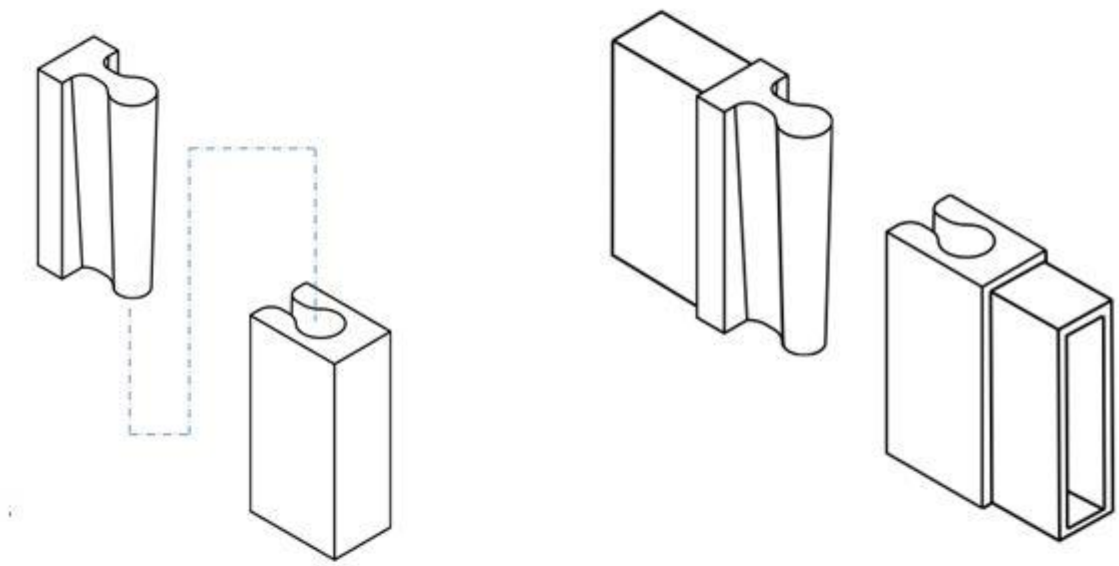

Figure 47: Design Assembly

Appendix C – Drawings

IN PROGRESS

Appendix D – Sample Calculations

Overall Bending Stress

Reaction Force:

$$R = \frac{P}{2} \quad (1)$$

Sample Calculation for the reaction force

$$R = \frac{175lb}{2} = 87.5\ lbs$$

Maximum Shear:

$$V_{max} = \pm\frac{P}{2} \quad (2)$$

Sample Calculation of the maximum shear

$$V_{max} = \pm\frac{175lb}{2} = \pm 87.5\ lbs$$

Maximum Moment:

$$M_{max} = \frac{PL}{4} \quad (3)$$

Sample Calculation of the maximum moment

$$M_{max} = \frac{(175lb)(20ft)\left(12\,{}^{in}/_{ft}\right)}{4} = 10{,}500\ lbs \cdot in$$

Overall Bending Stress

$$\sigma = \frac{Mc}{I} \quad (4)$$

Sample Calculation of Overall Bending Stress

$$\sigma = \frac{(21000lb-in)(1.625in)}{1.326in^4} = 25.7\ ksi$$

Deflection

Maximum Deflection:

$$\boldsymbol{\delta_{max}} = \frac{\boldsymbol{PL^3}}{\boldsymbol{48EI_x}} \quad (5)$$

Sample Calculation of the maximum deflection

$$\delta_{max} = \frac{(175lb)\left[(10ft)\left(12{}^{in}/_{ft}\right)\right]^3}{48(24\times10^6\frac{lb}{in^2})(1.326in^4)} = 0.198\ in$$

$$\delta_{max} = \frac{(175lb)\left[(20ft)\left(12{}^{in}/_{ft}\right)\right]^3}{48(24\times10^6\frac{lb}{in^2})(1.326in^4)} = 1.58\ in$$

Note: Modulus of Elasticity for carbon fiber was determined using a combination of composite spec sheet, Dr. George Staab and www.christinedemerchant.com/youngsmodulus.html

Bending – Joint

Necking

$$\sigma_{neck} = \frac{F}{A} \quad (6)$$

Sample calculation of necking

$$F = \frac{M}{2d} = \frac{10500\ lbs - in}{2(0.75\ in)} = 7000\ lbs$$

$$\sigma_{neck} = \frac{7000\ lbs}{(0.3\ in)(0.75\ in)} = 31.1\ \ ksi$$

$$n = \frac{S_u}{\sigma_{neck}} = \frac{71\ ksi}{31\ ksi} = 2.3$$

Bending – Single Component

Bending Stress of Rail in Single Component:

$$\sigma_{Rail} = \frac{M_{max} c_y}{I_x} \quad 7$$

Sample Calculation of Bending Stress of Rail in Single Component

$$\sigma_{Rail} = \frac{(10500\ lbs)(1.625\ in)}{1.326 in^4}$$

$$\sigma_{Rail} = 12.9\ ksi$$

Bending Stress of Rung in Single Component:

$$\sigma_{Rung} = \frac{M_{max} c_x}{I_y} \quad 8$$

Sample Calculation of Bending Stress of Rung in Single Component

$$\sigma_{Rung} = \frac{(10500\ lbs)(0.625\ in)}{0.279\ in^4}$$

$$\sigma_{Rung} = 23.5\ ksi$$

Horizontal Buckling – Locally

Local Horizontal Buckling

$$F_{crit} = \frac{K_h}{{L_e}^2}\sqrt{EI_yGJ_e} \quad 9$$

Sample Calculation of Local Horizontal Buckling in the Rung

$$J_e = \frac{hb^3}{3}$$

$$J_e = \frac{(1.25)(0.125)^3}{3} = 8.14 \times 10^{-4}\ in^4$$

$$I_y = \frac{1}{12}[hb^3]$$

$$I_y = \frac{1}{12}[1.25(0.125)^3]$$

$$I_y = 2.03 \times 10^{-4} in^4$$

$$F_{crit} = \frac{16.93}{(0.625in)^2}\sqrt{(580 \times 10^3\ {}^{lb}/_{in^2})(2.03 \times 10^{-4} in^4)(3.90 \times 10^6\ {}^{lb}/_{in^2})(8.14 \times 10^{-4}\ in^4)}$$

$$F_{crit} = 26.5\ kip$$

Sample Calculation of Local Horizontal Buckling in the Rail

$$J_e = \frac{bh^3}{3}$$

$$J_e = \frac{(0.125)(1.25)^3}{3} = 0.0814\ in^4$$

$$I_x = \frac{1}{12}[bh^3]$$

$$I_x = \frac{1}{12}[(0.125)(3.25)^3]$$

$$I_x = 0.358\ \text{in}^4$$

$$F_{crit} = \frac{16.93}{(1.625)^2}\sqrt{(580 \times 10^3\ {}^{lb}/_{in^2})(0.358\ in^4)(3.90 \times 10^6\ {}^{lb}/_{in^2})(0.0814\ in^4)}$$

$$F_{crit} = 1646\ kip$$

Vertical Buckling

Euler Equation for Vertical Buckling

$$F_{crit} = \frac{K_v}{{L_e}^2}\sqrt{EI_xGJ_e} \qquad (10)$$

Sample Calculations for Vertical Buckling

$$J_e = \frac{bh^3}{3}$$

$$J_e = \frac{(1.25)(3.25)^3}{3} = 14.3\ in^3$$

$$I_x = \frac{1}{12}[bh^3]$$

$$I_x = \frac{1}{12}[(1.25)(3.25)^3]$$

$$I_x = 3.58\ \text{in}^4$$

$$F = \frac{16.93}{\left[(2)(10ft)(12^{in}/_{ft})\right]^2}\sqrt{(580\times10^3\ lb/in^2)\,(3.58in^4)(3.90\times10^6)(14.3\ in^3)}$$

$$F = 3.16\ kip$$

Shear - Pin

Shear in Pin

$$V_{pin} = \frac{P}{A_{pin}} \qquad (11)$$

Sample Calculations of Shear in Pin

$$A_{pin} = \frac{\pi}{2}dh$$

$$A_{pin} = \frac{\pi}{2}(0.233)(0.375) = 0.137in^2$$

$$V_{pin} = \frac{P}{A_{pin}}$$

$$V_{pin} = \frac{350lb}{0.137in^2} = 2.55\ ksi$$

Shear - Adhesive

Shear in Adhesive Bonding

$$\tau_{max} = \kappa_s \tau_{ave} = \kappa_s \left(\frac{P}{bL_L}\right) \tag{12}$$

Sample Calculations of Shear in Adhesive Bonding

$$\tau_{max} = \kappa_s \tau_{ave} = \kappa_s \left(\frac{P}{bL_L}\right)$$

$$\tau_{max} = 2 \left(\frac{250\ lb}{(2.75\ in)(1.875\ in)}\right)$$

$$\tau_{max} = 97\ psi$$

Carbon Fiber Tube Dimension Determinacy Table

Variation	b (in)	h (in)	t (in)	c (in)	Iy (in^4)	Ix (in^4)	20 ft Stress (psi)	Does it Yield (20 ft)
Custom	1.250	3.250	0.125	1.625	0.279	1.326	25738	No
1	1.000	1.000	0.075	0.500	0.040	0.040	263602	No
2	1.000	1.000	0.100	0.500	0.049	0.049	213415	No
3	1.000	1.000	0.125	0.500	0.057	0.057	184320	No
4	1.000	1.250	0.075	0.625	0.048	0.068	191658	No
5	1.000	1.250	0.100	0.625	0.059	0.086	153356	No
6	1.000	1.250	0.125	0.625	0.069	0.100	130909	No
7	1.000	1.500	0.075	0.750	0.056	0.107	147233	No
8	1.000	1.500	0.100	0.750	0.070	0.135	116854	No
9	1.000	1.500	0.125	0.750	0.081	0.159	98945	No
10	1.000	1.750	0.075	0.875	0.064	0.156	117426	No
11	1.000	1.750	0.100	0.875	0.080	0.198	92636	No
12	1.000	1.750	0.125	0.875	0.093	0.236	77967	No
13	1.000	2.000	0.075	1.000	0.072	0.218	96252	No
14	1.000	2.000	0.100	1.000	0.090	0.278	75576	No
15	1.000	2.000	0.125	1.000	0.105	0.332	63309	No
16	1.000	2.250	0.075	1.125	0.080	0.293	80568	No
17	1.000	2.250	0.100	1.125	0.100	0.375	63021	No
18	1.000	2.250	0.125	1.125	0.117	0.449	52591	No
19	1.000	2.500	0.075	1.250	0.088	0.383	68571	No
20	1.000	2.500	0.100	1.250	0.110	0.491	53468	No
21	1.000	2.500	0.125	1.250	0.129	0.590	44479	No
22	1.000	2.750	0.075	1.375	0.096	0.488	59157	No
23	1.000	2.750	0.100	1.375	0.120	0.628	46005	No
24	1.000	2.750	0.125	1.375	0.141	0.757	38169	No
25	1.000	3.000	0.075	1.500	0.104	0.610	51616	No

26	1.000	3.000	0.100	1.500	0.131	0.787	40049	No
27	1.000	3.000	0.125	1.500	0.153	0.950	33151	No
28	1.250	1.000	0.075	0.500	0.068	0.048	219335	No
29	1.250	1.000	0.100	0.500	0.086	0.059	176867	No
30	1.250	1.000	0.125	0.500	0.100	0.069	152151	No
31	1.250	1.250	0.075	0.625	0.081	0.081	161157	No
32	1.250	1.250	0.100	0.625	0.102	0.102	128477	No
33	1.250	1.250	0.125	0.625	0.120	0.120	109268	No
34	1.250	1.500	0.075	0.750	0.094	0.126	124972	No
35	1.250	1.500	0.100	0.750	0.119	0.159	98855	No
36	1.250	1.500	0.125	0.750	0.140	0.189	83421	No
37	1.250	1.750	0.075	0.875	0.107	0.183	100519	No
38	1.250	1.750	0.100	0.875	0.135	0.232	79056	No
39	1.250	1.750	0.125	0.875	0.160	0.277	66331	No
40	1.250	2.000	0.075	1.000	0.120	0.253	83025	No
41	1.250	2.000	0.100	1.000	0.152	0.323	65009	No
42	1.250	2.000	0.125	1.000	0.180	0.387	54303	No
43	1.250	2.250	0.075	1.125	0.133	0.338	69980	No
44	1.250	2.250	0.100	1.125	0.168	0.433	54599	No
45	1.250	2.250	0.125	1.125	0.200	0.520	45445	No
46	1.250	2.500	0.075	1.250	0.146	0.438	59936	No
47	1.250	2.500	0.100	1.250	0.185	0.563	46626	No
48	1.250	2.500	0.125	1.250	0.219	0.678	38695	No
49	1.250	2.750	0.075	1.375	0.159	0.555	52008	No
50	1.250	2.750	0.100	1.375	0.202	0.715	40358	No
51	1.250	2.750	0.125	1.375	0.239	0.864	33410	No
52	1.250	3.000	0.075	1.500	0.172	0.690	45619	No
53	1.250	3.000	0.100	1.500	0.218	0.892	35326	No
54	1.250	3.000	0.125	1.500	0.259	1.079	29182	No
55	1.500	1.000	0.075	0.500	0.107	0.056	187799	No
56	1.500	1.000	0.100	0.500	0.135	0.070	151007	No
57	1.500	1.000	0.125	0.500	0.159	0.081	129542	No
58	1.500	1.250	0.075	0.625	0.126	0.094	139031	No
59	1.500	1.250	0.100	0.625	0.159	0.119	110544	No
60	1.500	1.250	0.125	0.625	0.189	0.140	93767	No
61	1.500	1.500	0.075	0.750	0.145	0.145	108559	No
62	1.500	1.500	0.100	0.750	0.184	0.184	85660	No
63	1.500	1.500	0.125	0.750	0.218	0.218	72107	No
64	1.500	1.750	0.075	0.875	0.164	0.209	87867	No
65	1.500	1.750	0.100	0.875	0.208	0.267	68949	No
66	1.500	1.750	0.125	0.875	0.248	0.318	57718	No
67	1.500	2.000	0.075	1.000	0.183	0.288	72995	No
68	1.500	2.000	0.100	1.000	0.233	0.368	57034	No

69	1.500	2.000	0.125	1.000	0.278	0.442	47540	No
70	1.500	2.250	0.075	1.125	0.202	0.382	61851	No
71	1.500	2.250	0.100	1.125	0.257	0.491	48163	No
72	1.500	2.250	0.125	1.125	0.307	0.590	40009	No
73	1.500	2.500	0.075	1.250	0.221	0.493	53233	No
74	1.500	2.500	0.100	1.250	0.282	0.635	41336	No
75	1.500	2.500	0.125	1.250	0.337	0.767	34242	No
76	1.500	2.750	0.075	1.375	0.240	0.622	46400	No
77	1.500	2.750	0.100	1.375	0.307	0.803	35946	No
78	1.500	2.750	0.125	1.375	0.367	0.972	29707	No
79	1.500	3.000	0.075	1.500	0.259	0.771	40871	No
80	1.500	3.000	0.100	1.500	0.331	0.997	31599	No
81	1.500	3.000	0.125	1.500	0.396	1.209	26062	No
82	1.750	1.000	0.075	0.500	0.156	0.064	164191	No
83	1.750	1.000	0.100	0.500	0.198	0.080	131744	No
84	1.750	1.000	0.125	0.500	0.236	0.093	112783	No
85	1.750	1.250	0.075	0.625	0.183	0.107	122248	No
86	1.750	1.250	0.100	0.625	0.232	0.135	97004	No
87	1.750	1.250	0.125	0.625	0.277	0.160	82118	No
88	1.750	1.500	0.075	0.750	0.209	0.164	95956	No
89	1.750	1.500	0.100	0.750	0.267	0.208	75573	No
90	1.750	1.500	0.125	0.750	0.318	0.248	63496	No
91	1.750	1.750	0.075	0.875	0.235	0.235	78045	No
92	1.750	1.750	0.100	0.875	0.301	0.301	61133	No
93	1.750	1.750	0.125	0.875	0.360	0.360	51084	No
94	1.750	2.000	0.075	1.000	0.262	0.322	65126	No
95	1.750	2.000	0.100	1.000	0.335	0.413	50802	No
96	1.750	2.000	0.125	1.000	0.401	0.497	42275	No
97	1.750	2.250	0.075	1.125	0.288	0.426	55414	No
98	1.750	2.250	0.100	1.125	0.369	0.548	43084	No
99	1.750	2.250	0.125	1.125	0.442	0.661	35734	No
100	1.750	2.500	0.075	1.250	0.314	0.548	47879	No
101	1.750	2.500	0.100	1.250	0.403	0.707	37125	No
102	1.750	2.500	0.125	1.250	0.484	0.855	30708	No
103	1.750	2.750	0.075	1.375	0.341	0.689	41884	No
104	1.750	2.750	0.100	1.375	0.437	0.891	32403	No
105	1.750	2.750	0.125	1.375	0.525	1.080	26742	No
106	1.750	3.000	0.075	1.500	0.367	0.851	37017	No
107	1.750	3.000	0.100	1.500	0.471	1.102	28584	No
108	1.750	3.000	0.125	1.500	0.566	1.338	23545	No
109	2.000	1.000	0.075	0.500	0.218	0.072	145855	No
110	2.000	1.000	0.100	0.500	0.278	0.090	116840	No
111	2.000	1.000	0.125	0.500	0.332	0.105	99864	No

112	2.000	1.250	0.075	0.625	0.253	0.120	109080	No
113	2.000	1.250	0.100	0.625	0.323	0.152	86419	No
114	2.000	1.250	0.125	0.625	0.387	0.180	73043	No
115	2.000	1.500	0.075	0.750	0.288	0.183	85975	No
116	2.000	1.500	0.100	0.750	0.368	0.233	67611	No
117	2.000	1.500	0.125	0.750	0.442	0.278	56722	No
118	2.000	1.750	0.075	0.875	0.322	0.262	70197	No
119	2.000	1.750	0.100	0.875	0.413	0.335	54908	No
120	2.000	1.750	0.125	0.875	0.497	0.401	45818	No
121	2.000	2.000	0.075	1.000	0.357	0.357	58789	No
122	2.000	2.000	0.100	1.000	0.459	0.459	45798	No
123	2.000	2.000	0.125	1.000	0.552	0.552	38060	No
124	2.000	2.250	0.075	1.125	0.392	0.471	50191	No
125	2.000	2.250	0.100	1.125	0.504	0.606	38974	No
126	2.000	2.250	0.125	1.125	0.607	0.732	32285	No
127	2.000	2.500	0.075	1.250	0.427	0.603	43503	No
128	2.000	2.500	0.100	1.250	0.549	0.779	33692	No
129	2.000	2.500	0.125	1.250	0.662	0.943	27836	No
130	2.000	2.750	0.075	1.375	0.461	0.757	38169	No
131	2.000	2.750	0.100	1.375	0.594	0.979	29496	No
132	2.000	2.750	0.125	1.375	0.717	1.188	24316	No
133	2.000	3.000	0.075	1.500	0.496	0.931	33828	No
134	2.000	3.000	0.100	1.500	0.639	1.207	26093	No
135	2.000	3.000	0.125	1.500	0.772	1.467	21471	No

Carbon Fiber Tube Dimension Determinacy Equations

$$Inertia:\ I_x = \frac{1}{12}[(bh^3 - (b-2t)(h-2t)^3)]$$

$$Inertia:\ I_y = \frac{1}{12}[(hb^3 - (h-2t)(b-2t)^3)]$$

$$Stress:\ \sigma = \frac{Mc}{I}$$

$$M = 10ft \times 12\frac{in}{ft} \times 175lbs = 21{,}000\ in - lbs$$

$$c = \frac{h}{2}$$

Assault Climbing Device

ISE 682 – Autumn 2011

Rohit Abraham
Darren Darby
Ashley Purdy
Shaun Ward

Design Process

- Eliminate Lead Climber
- **Anchor Lead Climber**
- Accelerate Lead Climb
- Improve Troop Climb

Existing Powder Fasteners

- Pull trigger to release firing pin which strikes powder load
- Powder load ignites and burns
- Expanding gases drive piston down the barrel into the fastener
- After each shot, the piston is manually reset by pulling the barrel assembly forward

Our Design



Fastener

- Angle Clip Fastener Specs
  - Diameter: 0.152 inches
  - Minimum penetration: 1-1/8 inches
  - 3000 psi → 1688 lbs (tension), unrated (shear)
  - 4000 psi → 1544 lbs (tension), unrated (shear)
- Ideal For Urban Structures
  - Masonry, concrete, cement block, steel

Fastener Ideas and Equipment

Climbing method

- Lead climber shoots an anchor point into rock face
- Attaches pulley and rope to anchor point
- Company pulls on rope and climber ascends
- When climber reaches first anchor point, he attaches a safety to it

Climbing method

- Shoots another anchor point, transfers pulley and rope to second anchor point
- Pulled up to second anchor point. Attaches second safety. Detaches first safety
- The process is repeated

Climbing method

- The rope pulley system can be replaced with a jumar, a prusik knot or a rope ladder
- The rope in all those cases can be fed from below and can go through the L bracket
- A tall lead climber with a long reach will be ideal
- This will enable the anchor points to be spaced out better.
- The anchors can be about 5 feet apart. Around 12 anchor points will be used to climb 60 feet

Additional Uses

- Shelter construction
- Repair patches for holes in steel
- Anchor anywhere
  - Cuff detainees to control
- Hammer or Club